# INNERVATION PATTERNS OF HARP SEAL

# (*PAGOPHILUS GROENLANDICUS*) VIBRISSAL SENSORY SYSTEMS

A Thesis

by

ERIN ELIZABETH MATTSON

Submitted to the Office of Graduate and Professional Studies of
Texas A&M University
in partial fulfillment of the requirements for the degree of

MASTER OF SCIENCE

| | |
|---|---|
| Chair of Committee, | Christopher D. Marshall |
| Committee Members, | Anja Schulze |
| | Bernd G. Würsig |
| Head of Department, | Anna R. Armitage |

December 2015

Major Subject: Marine Biology

## ABSTRACT

Vibrissae, or whiskers, are largest among pinnipeds and are specialized hairs that potentially evolved to serve sensory, thermoregulatory or protective functions. Behavioral data from pinniped and rodent vibrissa studies indicate that functional differences exist between medial microvibrissae and lateral macrovibrissae. However, comparative data are lacking, and current pinniped studies only focus on the largest ventrolateral macrovibrissae. Consequently, we investigated the medial-to-lateral innervation and microanatomy of harp seal (*Pagophilus groenlandicus*) vibrissal Follicle-Sinus Complexes (F-SCs). F-SCs were sectioned either longitudinally or in cross-section. Sections remained unstained or were stained with a modified Bodian silver stain (innervation) or Masson's trichrome stain (microanatomy). Harp seals possessed 88-105 F-SCs and each exhibited a tripartite blood organization system. Hair shafts were more circular medially but became more elliptical laterally. Medial F-SCs had more symmetrical dermal capsule thicknesses and distributions of major branches of the deep vibrissal nerve, but these symmetries diminished as F-SCs became more lateral. Medial-to-lateral axon counts ranged from 550 ± 97.4 axons/F-SC (medial) to 1632 ± 173.2 axons/F-SC (lateral). Overall, axon counts averaged 1221 ± 422.3 axons/F-SC (n=146 cross-sections), indicating a total of 117,235 axons/snout. Lateral F-SCs alone possessed a mean of 1533 ± 192.9 axons (n=82 cross-sections), which is similar to counts reported in other pinniped vibrissal innervation studies. These data suggest that conventional studies that only examine lateral vibrissae overestimate total innervation by

~20%. Moreover, we counted axon bundles with and without silver staining (n=834) and determined that unstained sections yielded more accurate and ~10% greater axon counts. Consequently, conventional analyses are likely only overestimating innervation by ~10% overall. The relationship between axon count and F-SC surface area was non-linear ($p<<0.01$; n=24 cross-sections), presumably from mechanoreceptors reaching carrying capacity, and axon densities were consistent across the snout. Presumptive Merkel-Neurite complexes and lanceolate endings were observed at the glassy membrane and outer root sheath interface. Our data agree well with behavioral research on pinnipeds and rodents that documents functional compartmentalization between micro-(medial) and macrovibrissae (lateral). Furthermore, our results support that vibrissal innervation variation observed among extant mammals initially diverged as a result of phylogeny and then environment (i.e., terrestrial, semi-aquatic, fully aquatic).

## DEDICATION

I dedicate my thesis to God and my family - even though all I have to offer is a one hundred-page paper about whiskers.

## ACKNOWLEDGMENTS

I thank Dr. Roger Reep for encouraging me to pursue graduate school in the first place and for reaching out to potential advisors. I will forever be grateful to him for helping me participate in his Veterinary Neuroscience course and setting up accommodations for me while I was in Florida. I also thank my committee chair, Dr. Christopher Marshall, for fostering my interest in neuroscience and marine biology. His financial support and ever-available advice have been instrumental in the completion of my Master's degree and thesis. Ich bedanke mich auch herzlich bei meinen beratenden Ausschuss-Mitgliedern, Dr. Anja Schulze und Dr. Bernd Würsig. Ihre Unterstützung und Kommentare waren sehr hilfreich und haben meine Abschlussarbeit erfreulich gemacht.

I am extremely indebted to Dr. Blair Sterba-Boatwright, who provided phenomenal, unfailing statistical guidance and support. He is the only teacher who could make me believe that I understand statistics. In addition, I am grateful for both the financial and logistical support provided by the Marine Biology department at Texas A&M University at Galveston, as well as the financial support of the Texas Institute of Oceanography, the Lerner-Gray Memorial Fund, and Texas Sea Grant that helped bring this research to fruition. This project would not have been possible without the help of Dr. Frank Fish and Carly Ginter-Summarell to secure whisker samples. Moreover, I thank Lauren Rust from The Marine Mammal Center in Sausalito for allowing me to visit the facility and aiding in my research.

Finally, I gratefully acknowledge my colleagues at Texas A&M who helped keep me sane throughout my two and a half years of research and late-night lab and writing sessions. Notably, I thank Dara Orbach, who has always encouraged me through difficult times in my research and given me the extra motivation and confidence to pursue great research and conference opportunities. A special thanks goes to the undergraduate students in the lab, who always maintained a positive attitude and helped me process samples despite the fact that I frequently started statements with, “I swear this is the last whisker . . .”

## NOMENCLATURE

| | |
|---|---|
| CT | Collagenous Trabeculae |
| DC | Dermal Capsule |
| DVN | Deep Vibrissal Nerve |
| F-SC | Follicle-Sinus Complex |
| GM | Glassy Membrane |
| HP | Hair Papilla |
| HS | Hair Shaft |
| ICB | Inner Conical Body |
| ICC | Intra-Class Correlation |
| IRS | Inner Root Sheath |
| LCS | Lower Cavernous Sinus |
| MNC | Merkel-Neurite Complex |
| MS | Mesenchymal Sheath |
| mya | Million Years Ago |
| ORS | Outer Root Sheath |
| RS | Ring Sinus |
| RW | Ringwulst |
| SD | Standard Deviation |
| SG | Sebaceous Glands |
| UCS | Upper Cavernous Sinus |

## TABLE OF CONTENTS

Page

## LIST OF FIGURES

## LIST OF TABLES

# 1. INTRODUCTION

The clade Pinnipedia consists of phocids (true seals), otariids (sea lions and fur seals), and odobenids (walruses). Pinnipeds possess the largest and most-developed vibrissae (whiskers), and these sensitive structures allow pinnipeds to detect vibrotactile cues and hunt successfully in diverse foraging niches [Huber, 1930a; 1930b; Ling, 1977; Dehnhardt et al., 2001; Marshall et al., 2006; Hanke et al., 2013; McGovern et al., 2015]. Pinniped diet is challenging to study due to numerous factors such as regional and seasonal variations in prey abundance, long-term changes in prey species composition, prey spawning and migration times, pinniped reproduction and molting periods, and differences in pinniped age and experience level [Adam and Berta, 2002; Lundström et al., 2010]. Captive tactile performance studies, animal-borne video recordings, stomach content and fecal analyses, and stable isotope data offer valuable information about pinniped diet and/or how pinnipeds utilize their vibrissae to forage [Kastelein and van Gaalen, 1988; Dehnhardt, 1994; Dehnhardt and Dücker, 1996; Lindstrøm et al., 1998; Parrish et al., 2000; Wathne et al., 2000; Dehnhardt et al., 2001; Adam and Berta, 2002; Davis et al., 2004; Greaves et al., 2004; Lundström et al., 2010; Wieskotten et al., 2010; Gläser et al., 2011; Labansen et al., 2011; Kernaléguen et al., 2012; Hanke et al., 2013; Grant et al., 2013; Heaslip et al., 2014]. However, analyzing innervation investment (i.e., innervation pattern, number and density of axons, and distribution of innervation) in the laboratory allows for greater sample sizes and is relatively quick and cost-effective. This method has been proposed as a proxy for sensitivity performance for several vertebrates

and can also convey information regarding a species' foraging strategy [Reep et al., 2001; Marshall et al., 2006; Hyvärinen et al., 2009; George and Holliday, 2013; Marshall et al., 2014a].

Investigations of the functional morphology, biomechanics, and innervation of pinniped vibrissae complements performance studies, thus allowing for an integrated understanding of pinniped sensory perception and hunting strategies that would not otherwise be possible [Marshall et al., 2006; Hanke et al., 2013]. However, a lack of comparative data on the microanatomy, innervation patterns, and degree of vibrissae innervation among pinnipeds has prevented more detailed ecological or evolutionary inferences. My research focuses on the neural organization of harp seal, *Pagophilus groenlandicus*, vibrissae. Consequently, we can draw conclusions about how harp seals use their vibrissae in nature, contribute to the growing literature regarding the evolution of vibrissal systems in fully aquatic mammals, and use harp seals to infer vibrissal function in similar phocids.

## 1.1 *Pinniped Vibrissae and Foraging Strategies*

Pinnipeds possess mystacial (upper lip), rhinal (on the rostrum), and supraorbital (above the eyes) vibrissae; however, otariids and odobenids lack rhinal vibrissae [Ling, 1977]. Throughout this thesis, "mystacial array" refers to all mystacial vibrissae on an individual (i.e., both sides of the muzzle), while "mystacial field" or "mystacial pad" only includes the unilateral group of mystacial vibrissae on an individual (i.e., one side of the muzzle). Vibrissae vary in number, geometric arrangement, size, shape, flexural

stiffness, and innervation [Ling, 1977; Ginter et al., 2010; 2012; Hanke et al., 2013; Ginter-Summarell et al., 2015]. In general, a pinniped's vibrissal function and sensory perception is believed to be categorized by its dominant hunting mode. A dichotomy appears to exist between hydrodynamic trail following and active touch, but all pinnipeds retain both capabilities to some extent. Recent data suggest that, during foraging, most phocids rely predominantly on following hydrodynamic wake trails left by prey within the water column, whereas otariids and odobenids depend more on active touch sensation (haptics) in benthic habitats [Ling, 1972; Kastelein and van Gaalen, 1988; Dehnhardt, 1994; Dehnhardt and Dücker, 1996; Dehnhardt et al., 2001; Berta et al., 2006; Marshall et al., 2006; Ginter et al., 2012; Hanke et al., 2013]. Otariids, specifically California sea lions (*Zalophus californianus*), can still follow hydrodynamic trails, but their performance (success rate) relative to harbor seals (*Phoca vitulina*) is reduced [Gläser et al., 2011].

This foraging-based dichotomy is likely due to a myriad of variables, but one crucial element that is emerging is vibrissal hair shaft (HS) morphology. Most pinniped vibrissae HSs exhibit flattened, elliptical cross-sections, rather than the circular cross-sections observed in terrestrial and semi-aquatic mammals, sea otters (*Enhydra lutris*), West Indian Florida manatees (*Trichechus manatus latirostris*), and cetaceans [Dehnhardt et al., 1999; Reep et al., 2001; Hyvärinen et al., 2009; Miersch et al., 2011; Hanke et al., 2013; Marshall et al., 2014a; Drake et al., 2015; Berta et al., 2015]. Aside from the elliptical design, the absence or presence of beading along the HS (Figure 1) is also fundamental to the partition, with some exceptions. Beaded HSs are typically seen

in hydrodynamic trail-following phocids, but, according to some studies, they are not present in bearded (*Erignathus barbatus*), Ross (*Ommatophoca rossii*), leopard (*Hydrurga leptonyx*), and monk seals (*Neomonachus sp.*). In general, predominantly benthic-foraging pinnipeds do not have beaded HSs. [Ling, 1972; 1977; Berta et al., 2006; Marshall et al., 2006; Ginter et al., 2010; 2012]. Computational fluid dynamic models showed that elliptical, beaded HSs appear to reduce the background water "noise" caused by swimming, thereby allowing harbor seals to detect prey wake trails with greater sensitivity [Hanke et al., 2010]. However, a similar study showed that only the elliptical characteristic was responsible for dampening vibrissal vortices and that the function of the HS beads was still unclear, but the researchers hypothesized that the beads could aid in filtering or amplifying specific types of hydrodynamic stimuli [Murphy et al., 2013]. In addition, the researchers noted that elliptical HS flattening became more pronounced towards the vibrissal tip, regardless of a beaded or smooth profile [Murphy et al., 2013]. In essence, the variation seen in HS design likely correlates to differences in pinniped hydrodynamic perception and prey preferences, but other factors, such as orofacial morphology and mystacial field location on the muzzle, may also be important [Marshall et al., 2006; Hanke et al., 2010; 2013]. From these data, it seems probable that pinniped vibrissae are functionally "tuned" to their respective foraging niche [Marshall et al., 2006; Hanke et al., 2013].

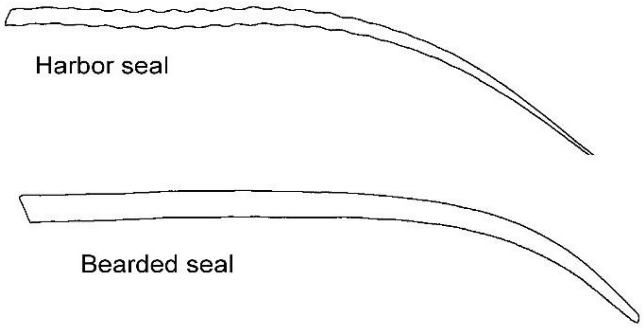


**Figure 1. Example outlines of vibrissal hair shafts from two phocid species.** Top: Beaded vibrissa from a wake trail-following harbor seal. Bottom: Smooth vibrissa from a benthic-foraging bearded seal [Ginter et al., 2012][*].

1.1a *Harp Seal Vibrissae, Foraging Strategies, and Diet*

Harp seals, similar to other phocids, molt their pelage hair synchronously but shed and replace their vibrissae asynchronously, presumably to ensure that they always retain high levels of sensory perception [Hirons et al., 2001; Greaves et al., 2004]. Harp seals are reported to possess a maximum of 49 vibrissae per mystacial pad. Subtle differences in vibrissal distribution may exist between sexes or age groups in harp seals [Yablokov and Klevezal, 1962]. However, this variation is likely natural, due to small sample sizes, or the result of human error because mammals are born with a finite number of hair follicles and nerve fibers (axons) innervating them. Axons will only vary in their degree of myelination, a process that continues throughout life [Szabo, 1958; Winkelmann, 1959; Scheffer, 1964; Reep et al., 2002; Setzu et al., 2004; Ito et al., 2007].

[*] Reprinted under the Creative Commons Attribution license of PLoS ONE.

Harp seals are similar to harbor seals in their generalist-foraging strategy. Both possess beaded HSs and fall into the hydrodynamic perception category during hunting [Ginter et al., 2010; 2012]. In respect to HS design, harp and harbor seals have almost identical vibrissal HS crest and trough widths means, which contribute to their similar foraging strategies [Ginter et al., 2010; 2012; Hanke et al., 2013]. To optimize foraging, pinnipeds must consider several factors such as dive time, prey size, search time, and prey energy intake [Stephens and Krebs, 1986; Bowen et al., 2002; Stephens et al., 2008]. These consideration are more straightforward for generalist foragers (e.g., Australian fur seals [*Arctocephalus pusillus*] and harbor, harp, and ringed seals[*Pusa hispidia*]) because they can exploit a variety of feeding modalities and environmental niches, consequently adapting well to an array of environmental conditions [Wathne et al., 2000; Marshall et al., 2006; Labansen et al., 2011; Ginter et al., 2012; Hanke et al., 2013; Hocking et al., 2013; 2014; Marshall et al., 2014b]. Four pinniped feeding modalities have been proposed [i.e., bite, suction, filter, grip-and-tear; Adam and Berta, 2002]. Many pinnipeds, such as Steller sea lions (*Eumetopias jubatus*), bearded seals, harbor seals, Australian fur seals, and leopard seals, can switch between two or more feeding modalities [Marshall et al., 2008; Hocking et al., 2013; 2014; Marshall et al, 2014b; in press; Marshall and Goldbogen, in press]. For example, harbor seals predominantly utilize suction but will also incorporate biting. In addition, they also exhibit hydraulic jetting to help dislodge difficult-to-acquire prey [Marshall et al., 2014b]. The absence of a strict adherence to one feeding modality among generalists is likely a shared trait and helps account for their diverse diets [Marshall et al., 2014b].

Since harp seals share similar vibrissal characteristics as harbor seals, these data support that harp seals are generalist foragers and are capable of using multiple feeding modes, but this generalization has yet to be examined directly.

Meta-analyses also indicate that harp seals are generalists. These analyses separate a pinniped's diet into four broad categories: benthic invertebrates and large zooplankton, cephalopods, fish, and higher vertebrates [e.g., marine mammals, seabirds, sea turtles; Pauly et al., 1998]. Harp seals consume a high percentage of fish (~70%) but can also forage in benthic locations (~25%). The remaining 5% of their diet usually consists of squid [Ridgway and Harrison, 1981; King, 1983; Riedman, 1990; Lydersen et al., 1991; Lindstrøm et al., 1998; further citations in Pauly et al., 1998]. Harp seal diet also varies by location and season [Beck et al., 1993; Nilssen, 1995; Nilssen et al., 2000]. For instance, migrating harp seals from the northern Gulf of St. Lawrence feed on a spectrum of invertebrates and fish [Beck et al., 1993]. Barents Sea harp seals forage mainly on capelin (*Mallolus villosus*), polar cod (*Boreogadus saida*), herring (*Clupea harengus*), cod (*Gadus morhua*), and amphipods (*Parathemisto libellula*), but preferences vary by season, with the seals favoring amphipods in the fall but switching to pelagic fish and crustaceans in the winter [Nilssen, 1995; Nilssen et al., 2000]. Barents Sea ringed and harp seals have an almost complete foraging niche overlap (0.985 overlap index), but the specific area they utilize within that niche may vary [Wathne et al., 2000]. These data further support that harp seals are generalist foragers, and it is probable that my harp seal findings can be applied to other generalist phocids.

## 1.2 *Vibrissae Microanatomy: The Follicle-Sinus Complex*

The blood-filled Follicle-Sinus Complex (F-SC) spans the epidermis, dermis, and hypodermis. This vital sensory organ transduces environmental vibrotactile stimuli received by the HS into action potentials that can be interpreted by the central nervous system [Ling, 1977; Rice et al., 1986; Ebara et al., 2002; Hanke et al., 2013]. F-SCs vary substantially in size and shape [Ling, 1977]. Mystacial F-SCs are the largest and are innervated by branches of the infraorbital nerve, a major nerve of the maxillary branch of the trigeminal nerve [Cranial nerve V; Ling, 1977]. A large infraorbital foramen, which is a cranial passageway for the blood vessels and axons that supply the rostrum and vibrissae, is a shared, defining characteristic of pinnipeds [Berta and Wyss, 1994; Hu et al., 2006].

For many species, the arrangement of vibrissae on the muzzle is expressed as a somatotopic map within the cerebral cortex [i.e., scaled projections of peripheral sensory areas in the central nervous system; Daniel and Whitteridge, 1961; Welker et al., 1964; Radinsky, 1968; Woolsey and Van der Loos, 1970; Nomura et al., 1986; Catania, 2007; Sarko et al., 2011]. The more important a tactile area is functionally, the larger it will be represented in the somatosensory cortex [i.e., cortical magnification; Daniel and Whitteridge, 1961; Catania, 2007]. Limited data from northern fur seals (*Callorhinus ursinus*) showed a greatly expanded representation of mystacial vibrissae within the somatosensory cortex [Ladygina et al., 1985]. All mystacial vibrissae, except the most dorsal row of vibrissae, were found to be projected onto the somatosensory cortex with similar surface areas, despite variations in vibrissa size. Therefore, it was suggested that

all mystacial vibrissae, excluding the most dorsal row, possess a comparable "functional load" [Ladygina et al., 1985]. From these data, and the similarity in cortical organization of vibrissae within several well-studied terrestrial species [Catania, 2012], we can infer that other pinnipeds likely have similarly organized somatosensory cortices. Trigeminal nerve terminations within the central nervous system are reasonably consistent among vertebrates. The cell bodies of the infraorbital nerve reside within the descending nucleus and principle nucleus (pons) of the trigeminal nerve [Butler and Hodos, 1996]. The entire trigeminal nuclear complex of phocids is regarded as the largest among carnivores [Ridgway and Harrison, 1981]. This suggests that phocids have increased vibrissal innervation compared to other pinnipeds but additional comparative neural data are needed.

The axons that relay the information from pinniped vibrissae to the somatosensory cortex can be non-myelinated or myelinated, slowly-adapting or rapidly-adapting Aβ, Aδ, and C afferent nerve fibers [Dykes, 1974; Fleming and Luo, 2013]. Because non-myelinated axons are less discernible, not much is known about how they terminate within F-SCs. However, among mammals, larger, myelinated axons appear to terminate mainly in lamellated corpuscles (acceleration, vibration detectors), free nerve endings (pain receptors), Ruffini's corpuscles (tension, stretch receptors), Merkel cell-neurite complexes (MNCs; pressure receptors), and lanceolate endings (velocity receptors). The majority of these mechanoreceptors are located at the level of the ring sinus (RS) on either side of the glassy membrane (GM) and form a ring around the HS [Andres, 1966; Ling, 1977; Gottschaldt et al., 1982; Rice et al., 1986; Halata, 1993;

Hyvärinen, 1995; Necker, 2000; Dehnhardt and Mauck, 2008]. The current functional hypothesis suggests that when the HS bends, the mesenchymal sheath (MS) compresses along the leading edge of the HS, consequently stretching the surrounding tissues and stimulating nearby mechanoreceptors [Rice et al., 1986; Lichtenstein et al., 1990; Dehnhardt et al., 1999].

### 1.3 *Vibrissae Innervation and Evolution*

The origin and selection pressures leading to the evolution of hair is a highly speculative topic due to lack of fossil evidence. However, it is suggested that hair evolved ~200 million years ago (mya) in early cynodonts (ancestors to modern mammals), approximately 150+ million years after vertebrates began to invade land [Meng and Wyss, 1997; Maderson, 2003; Ahlberg and Clark, 2006]. Some researchers posit that hair evolved from cutaneous or sebaceous glands [SG; Stenn et al., 2008; Dhouailly, 2009], while others suggest a re-appropriation of hair keratins (e.g., scales), since these structural proteins are not unique to mammals [Eckhart et al., 2008]. Another hypothesis is that hair evolved from modified mechanoreceptors [Maderson, 1972]. A newly revised theory now proposes that the mutation of a molecular trigger that was partly responsible for patterning genes resulted in the creation of mechanosensory "protohairs" and "protopelage" [Maderson, 2003].

The initial function of these "protohairs" could have been for protection or to help minimize cutaneous water loss as early amniotes ventured into terrestrial habitats and had to adapt to drier and more physically abrasive environments. Secondarily, the

hairs likely aided in thermoregulation and were a contributing factor in the development of endothermy millions of year later [Maderson, 1972; 2003]. However, because of the prominent morphological differences between pelage hair and vibrissae, some researchers think that pelage hair and vibrissae each arose independently. Subsequently, it has also been suggested that vibrissae evolved from mechanoreceptors for a sensory function, while pelage hair formed from the epidermis for thermoregulation [Chernova, 2006]. Most of these theories support the general assertion that vibrissae, not pelage hair, were the first to evolve. This hypothesis is further supported by the fact that, during embryonic development, vibrissae appear before pelage hair in most mammals, including pinnipeds [Hardy, 1951; Davidson and Hardy, 1952; Ling, 1977]. The terrestrial-aquatic transition of several mammalian lineages (e.g., Pinnipedia, Cetacea, Sirenia) likely placed strong selection pressures on vibrissal innervation, function, and morphology [Berta et al., 2006; Uhen, 2007; Marshall et al., 2014a].

It appears probable that vibrissae initially evolved to fulfill a strictly sensory role, while pelage hair developed more for thermoregulatory or skin protectant purposes. Since vibrissae have a sensory-specific function compared to pelage hair, they are primed to detect more spatially-oriented signals and probably underwent greater functional constraints as they evolved. Consequently, it makes sense that vibrissal innervation would be specifically adapted for a species' environment (i.e., terrestrial, semi-aquatic, fully aquatic) but would diminish if other modes of sensory perception were available (e.g., echolocation).

### 1.3a *Aquatic Transition of Pinniped Ancestors*

Pinnipeds are accepted as a monophyletic group, with mustelids or ursids (i.e., polar bears) being their closest relatives [Berta et al., 2006; Berta, 2009]. The origin of pinnipedimorphs (pinnipeds and their ancestors) is a speculative topic, since fossil evidence is sparse. However, fossils of *Enaliarctos* and *Pteronarctos,* discovered in late Oligocene (~27-20 mya) and early Miocene sediments (~19-15 mya), respectively, offer clues about their origin [Savage, 1957; Berta et al., 1989; Berta, 1991; Berta et al., 2006; Rybczynski et al., 2009; Kelley and Pyenson, 2015]. *Enaliarctos*, a fossil from the North Pacific, is the earliest recognized pinnipedimorph because of its short tail and well-developed flippers [Figure 2; Mitchell and Tedford, 1973; Berta et al., 1989; Berta, 1991; Berta et al., 2006; Rybczynski et al., 2009]. *Pteronarctos*, a fossil discovered in Oregon, is considered a pinnipedimorph but is more closely related to extant pinnipeds than *Enaliarctos* [Figure 2; Berta et al., 2006; Berta, 2009]. Although data are lacking, it is likely that pinnipeds underwent their aquatic transition in stages, beginning in freshwater before migrating to the open ocean [Berta et al., 1989; Rybczynski et al., 2009].

The origin of phocids may date back to the late Oligocene (~29-23 mya). Two partial femora, referred to as "Oligocene seal," share characteristics with modern phocids and, if correctly aged, would make the bones from the oldest known phocid and pinniped, even pre-dating *Enaliarctos* [Koretsky and Sanders, 2002; Berta et al., 2006]. The timeline of "Oligocene seal" is still disputed, but most researchers accept that monachines and phocines diverged between 22 and 15 mya [Figure 2; Arnason et al.,

2006; Berta, 2009]. It is also generally accepted that odobenids and otariids are monophyletic, sister groups [Berta et al., 2006; Berta, 2009; Berta and Churchill, 2012]. Timelines for the origin of odobenids and otariids in the fossil record are reasonably agreed upon. Odobenids arose during the middle Miocene (~16-14 mya) in the North Pacific, followed shortly after by otariids towards the end of the Miocene [~11 mya; Figure 2; Downs, 1956; Kohno et al., 1994; Deméré and Berta, 2002; Berta et al., 2006].

### 1.4 *Medial vs. Lateral Mystacial Vibrissae*

Differences in the microanatomy, function, and innervation between medial microvibrissae and lateral macrovibrissae have been noted in terrestrial, semi-aquatic, and some fully aquatic mammals [Lee and Woolsey, 1975; Rice et al, 1986; Marotte et al., 1992; Brecht et al., 1997; Dehnhardt et al., 1999; Hartmann, 2001; Reep et al., 2001; Hyvärinen et al., 2009], but these differences have yet to be systematically examined for pinnipeds. Semi-aquatic Australian water rats (*Hydromys chrysogaster*) are good microanatomical examples, as their macrovibrissae lack a ringwulst [RW; Dehnhardt et al., 1999]. A functional example would be that rodents and shrews mainly use their macrovibrissae in "whisking" behavior (i.e. rapidly sweeping vibrissae back and forth), but they deliberately place their microvibrissae on objects [Hartmann, 2001]. Another rat study showed that their macrovibrissae were essential distance indicators and important in spatial tasks but that they were superfluous for object recognition. In contrast, rat microvibrissae were vital for object recognition, but they did not contribute to spatial tasks [Brecht et al., 1997].

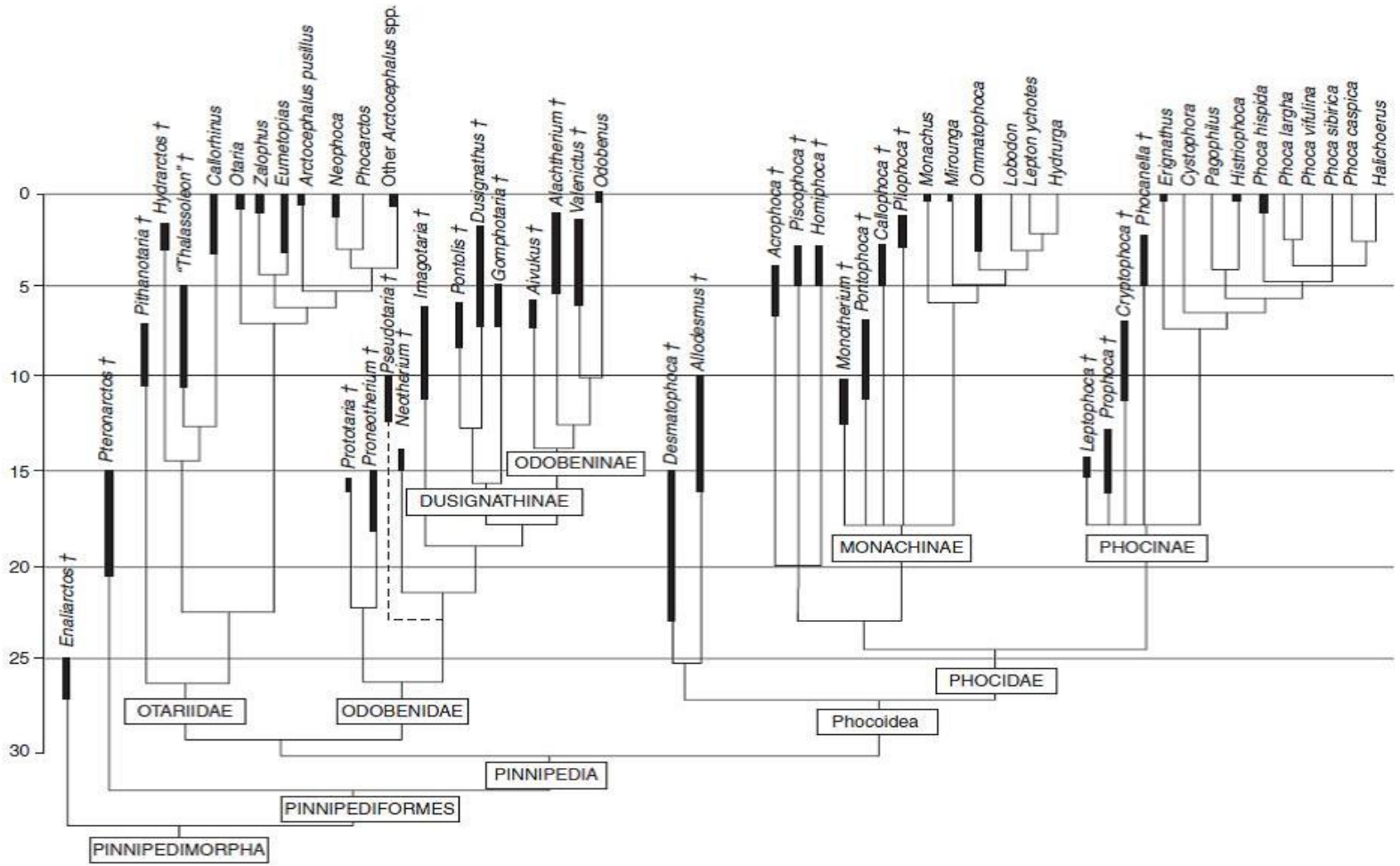


**Figure 2. Pinnipedimorpha cladogram.** Cladogram in mya showing the divergence of extinct and extant members of Pinnipedimorpha [Berta, 2009]*.

* Reprinted with permission from The Encyclopedia of Marine Mammals (2nd ed.), by Berta A, 2009, Academic Press, San Diego. Copyright 2009 by Elsevier Inc.

The behavioral use of macro- and microvibrissae during tactile sensitivity testing and feeding performance studies have been reported for walruses (*Odobenus rosmarus*), California sea lions, harbor seals, and bearded seals, but to date no data on the innervation and microstructure of pinniped microvibrissae exist. Behavioral, active-touch experiments on California sea lions, harbor seals, and walruses have shown that these pinnipeds initially contact objects with their lateral vibrissae and then reorient so that only their smaller, medial vibrissae are touching the object [Kastelein and van Gaalen, 1988; Dehnhardt and Dücker, 1996; Grant et al., 2013]. In addition, harbor seals prefer to localize objects on their most ventral, medial vibrissae [Grant et al., 2013]. Medial microvibrissae are short, small in diameter, and densely clustered together, apparently allowing for higher resolution power. As a result of these performance studies, it is suggested that harbor seals use the overall number of vibrissae touching an object as the primary indicator of size, rather than the position, angle, or spread of the vibrissae [Grant et al., 2013]. These studies provide behavioral support that suggests an underlying difference exists in the microanatomy and/or innervation patterns of medial and lateral vibrissae in pinnipeds, but no studies have investigated this or proposed a distinction between micro-(medial) and macrovibrissae (lateral) in pinnipeds.

## 1.5 *Objectives and Hypotheses*

Our research addresses gaps in data pertaining to pinniped vibrissal innervation investment, medial-to-lateral (micro- and macrovibrissae) axon counts and

microanatomy, and axon densities. Our objectives were to characterize harp seal vibrissal microanatomy and quantify F-SC innervation to test the following hypotheses:

*Hypothesis 1:* The number of axons in large, lateral vibrissae does not vary substantially among harp seals and other phocids.

*Hypothesis 2:* The total number of axons innervating the entire harp seal mystacial vibrissal array is less than values reported for other phocids when medial vibrissae are included.

*Hypothesis 3:* The number of axons per vibrissa shows a positive linear correlation with vibrissal surface area from small, medial vibrissae to large, lateral vibrissae.

# 2. MATERIALS AND METHODS

## 2.1 *Vibrissae Samples and Storage*

Eight harp seal vibrissal pads (left or right) from five seals were obtained from the Department of Marine Resources (Augusta, Maine), Marine Mammal Stranding Center (Brigantine, New Jersey), and the Marine Animal Rehabilitation and Conservation Program (Biddeford, Maine) under U.S. National Marine Fisheries Service Southeast Regional Office salvage permit #358-1585. Sample collection was opportunistic, but current literature demonstrates that innervation investment is independent of age class and sex [Winkelmann, 1959; Setzu et al., 2004; Ito et al., 2007; McGovern et al., 2015]. Vibrissal pads were collected within 72 hours postmortem, either initially fixed in 10% formaldehyde or frozen at -20$^{o}$C and then fixed in 10% formaldehyde until ready for processing. Although vibrissal pads had been frozen, once they were thawed and fixed in 10% phosphate-buffered formaldehyde the tissues were determined to be suitable for microanatomical characterization and innervation quantification. Previously frozen samples could be used because our research focused on the tissue microstructure, rather than the cellular level, which would require stricter cryopreservation protocols [Karlsson and Toner, 1996].

## 2.2 *Gross Vibrissal Morphometrics*

Maximum vibrissal span (length and width) across the pad was measured using digital calipers. Individual vibrissae were counted, and their position on the pad was

mapped (Figure 3). Five of the largest ventrocaudal vibrissae on each pad (i.e., “lateral vibrissae”), as well as successive vibrissae across the second most ventral row on each pad (i.e., “medial vibrissae”) were dissected. Ideally, every third vibrissa successively across the vibrissal pad would have been collected for the medial-to-lateral analysis. However, an even distribution of vibrissae across the vibrissal pad was not always feasible. Consequently, intermediate vibrissae were sometimes dissected to maintain an adequate sample size. Vibrissa morphometrics (i.e., HS length and diameters, upper cavernous sinus [UCS] and lower cavernous sinus [LCS] diameters, and F-SC length) were collected using digital calipers. Two diameter measurements, major and minor axes, were taken at the HS base. After measurements were recorded, the HS was cut at the follicle base and stored dry. The F-SCs were stored in 10% phosphate-buffered formaldehyde at room temperature until sectioned.

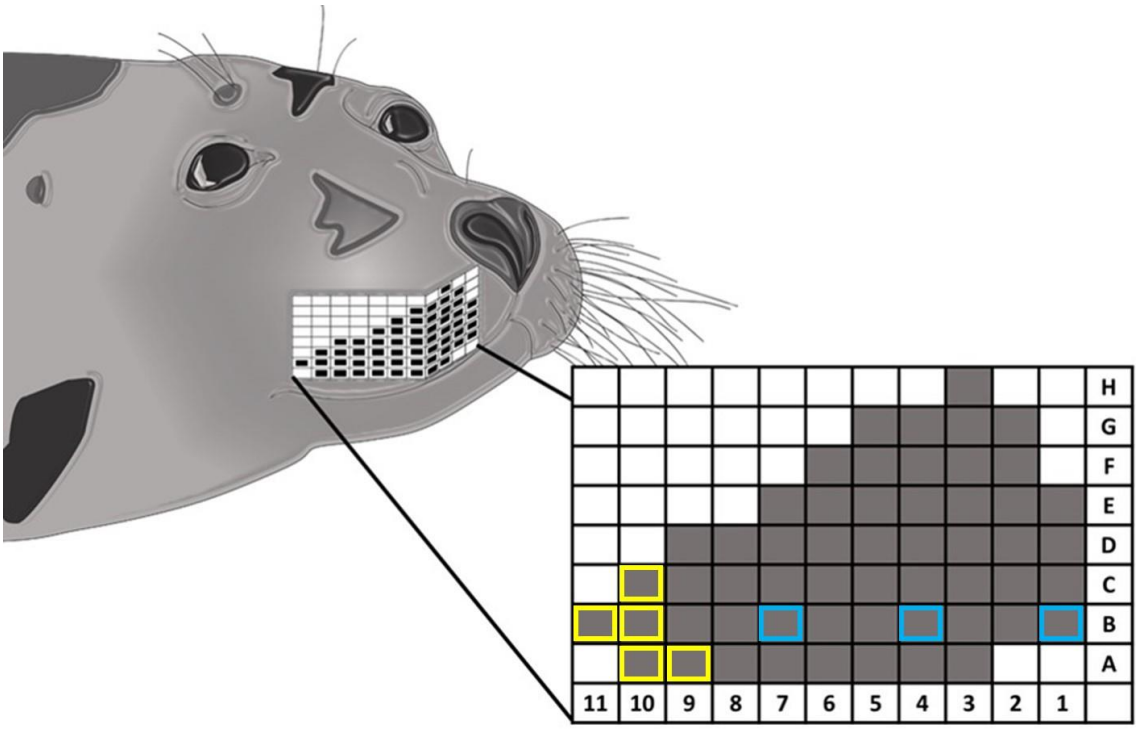


**Figure 3. Harp seal vibrissal map (including column and row labeling).** Shaded squares represent locations of vibrissae. Yellow-highlighted squares are representative of ventrocaudal, "lateral" vibrissae locations, while blue-highlighted squares show examples of "medial" vibrissae locations.

## 2.3 *Vibrissal Microstructure*

Three large, ventrocaudal vibrissae from each pad were sectioned on a Lipshaw 80A sliding-stage microtome (Detroit, Michigan) with a freezing stage attached (Physitemp Instruments, BFS Series, Clifton, New Jersey). Samples were sectioned both longitudinally and in cross-section at 25-30µm. Serial sections were mounted onto 1% gel slides using 0.9% phosphate-buffered saline. Three medial vibrissae (one column 2 vibrissa and two column 3 vibrissae) were also sectioned longitudinally. Longitudinal sections were stained with a modified Masson's trichrome [for overall microstructure;

Masson, 1929] or a modified Bodian silver stain [for deep vibrissal nerve (DVN) entry location and patterns of innervation; Bodian, 1936]. All cross-section microstructural morphometrics were measured from wet-mounted, unstained sections. Optimal sections for analysis were selected from mid-F-SC for longitudinal sections and from mid-LCS for cross-sections. A total of 19 and 24 F-SCs were analyzed for longitudinal and cross-section morphometrics, respectively. All measurements were performed in triplicate.

Micrographs were taken using a Pursuit Slider digital camera (Diagnostic Instruments Inc., USA) mounted on a Nikon SMZ1500 stereoscope (longitudinal sections), or mounted on a Nikon Eclipse E400 light microscope (cross-sections). Images were adjusted for brightness and contrast. The following morphometrics were collected: (1) maximum F-SC, UCS, RS, and LCS lengths, (2) maximum RS and dermal capsule (DC) widths, (3) total sinus length (i.e., UCS, RS, and LCS combined), and (4) percent of largest UCS, RS, and LCS length to the total F-SC length from longitudinal sections. SPOT advanced software was used to measure and/or determine the existence of the following structures from cross-sections: (1) maximum F-SC diameter, (2) HS area (including cortex and medulla), (3) F-SC area excluding the DC, (4) width of major and minor axes of HS, (5) the angle between the thinnest DC area and the F-SC's midline, (6) the angle between the thinnest DC location and the thickest DC location, (7) the thinnest, thickest, and representative widths of the MS, collagenous trabeculae (CT), and DC (8) RW, (9) inner conical body (ICB), (10) GM, (11) outer root sheath (ORS), (12) inner root sheath (IRS), (13) superficial vibrissal nerve, (14) MNCs, (15) hair papilla (HP), (16) SGs, and (17) F-SC dimple. The surface area measurement that was

used to determine vibrissal axon density was obtained by subtracting the measured HS surface area from the total F-SC area (excluding the DC). All aforementioned measurements were repeated in triplicate and the means were used for analyses.

### 2.4 *F-SC Innervation*

Innervation was quantified by conducting counts of myelinated axons from mid-LCS cross-sections using a Nikon Eclipse E400 light microscope at 40x. Counts were conducted at this location to be consistent with previous studies and allow for a direct comparison. Moreover, previous studies have also shown that axon branching is minimal prior to this location [Dehnhardt et al., 1999; Marshall et al., 2006; 2014a; McGovern et al., 2015]. Two large, ventrocaudal vibrissae per vibrissal pad, as well as successive vibrissae in the second most ventral row, were processed for axon counts. Adobe Photoshop was used to mark axons during counting to prevent under- or over-counting. Depending on image quality, between one and five cross-sections per F-SC were analyzed for axon counts. A total of 146 cross-sections were evaluated.

Initially, cross-sections were stained with a modified Bodian silver stain (following Reep *et al.* [2001], Marshall *et al.* [2006; 2014a], and McGovern *et al.* [2015]) to count axons. However, the staining process was inconsistent and unpredictable, rendering multiple sections unquantifiable. For a cross-section to meet our criteria for analysis, at least 90% of the CT and axon bundles needed to be intact and positively stained. These conditions were rarely satisfied with the silver-staining process. From personal observation, axon bundles usually appeared in good condition directly

after sectioning, and we were able to obtain high quality images for analysis from unstained, wet-mounted sections. Therefore we used unstained, wet-mounted cross-sections for axon quantification after extensive validation with stained vs. unstained sections of the same cross-section (see below).

### 2.5 *Wet vs. Stained Axon Count Comparison and Method Validation*

Forty-two cross-sections from nine vibrissae and three harp seals were processed for the axon count method comparison. Three separate readers counted ten axon bundles from each cross-section before and after staining (n=412 bundles). Technical difficulties prevented some images from being processed, and 13 cross-sections were lost during staining. Previous trials had shown that varying gel slide percentage, heating the slides, using electrostatic slides, and sectioning at different thickness resulted in no improvement in section adhesion. The use of a cyanoacrylate adhesive (i.e., Super Glue) on the outermost edge of the DC of several sections after mounting greatly improved tissue attachment without interfering with axon bundle quality. This method was adopted for the remainder of the cross-sections when staining.

For consistency, all readers used the same images for digital analyses but brightness and contrast could be adjusted. From the results, inter-reader (also referred to as inter-rater) reliability was assessed rather than percentage of agreement, because inter-reader reliability analyses account for chance agreement and provide more statistical information [Hallgren, 2012]. R (version 3.2.1) was used to conduct a two-way absolute single-measures Intra-Class Correlation (ICC) to assess inter-reader

reliability. ICC for readers when analyzing wet, unstained axon bundles was 0.966, with a 95% confidence interval of 0.960-0.971 (n=412, F-test p<<0.01), indicating excellent inter-reader reliability (ICC=1 is perfect agreement). Notably, only analyzing the first 200 wet bundle counts among readers still yielded an ICC of 0.960 (n=200, F-test $p=2.1^{-203}$, 95% confidence interval=0.949-0.968). Stained axon counts among readers produced a lower ICC of 0.945 and a wider 95% confidence interval of 0.920-0.961 (n=278, F-test $p=1.14^{-48}$), but this lower ICC was still indicative of excellent inter-reader reliability [Hallgren, 2012].

Paired Student's t-tests were conducted on each reader's counts to determine if there was a significant difference between their wet and stained counts (data met assumptions for the test). Two readers showed significant differences between techniques (n=278, $p=7.693^{-16}$ and $p<2.2^{-16}$). For both of these readers, their axon counts were found to be significantly higher in wet sections than in stained sections (n=278, $p=3.846^{-16}$ and $p<2.2^{-16}$). For the third counter, there was no significant evidence that axon counts varied before or after staining (n=278, p=0.121).

A linear mixed-effects model was conducted to determine overall differences between wet and stained counts among readers. Data met assumptions for the test, and reader was considered a random variable. More data points were present below a $45^{o}$ trendline (slope=1, intercept=0), indicating that readers usually counted fewer axons within the same bundle after staining (Figure 4). Minor heteroscedasticity within the data existed and was accounted for by using the *varPower* function on the model. The *varPower* adjustment resulted in a lower AICc value, but diagnostic plots showed that

some outliers were causing slight non-linearity within the model. Attempts to address the non-linearity with the use of a spline confounded the data past useful interpretation and this technique was therefore omitted. The *varPower* linear mixed-effects model was significant ($p<5x10^{-5}$) and was plotted by the equation: Stained Count=0.896(Wet Count) + 0.499 (Figure 5). In essence, this equation means that, on average, stained counts are 10.4% lower than wet measurements.

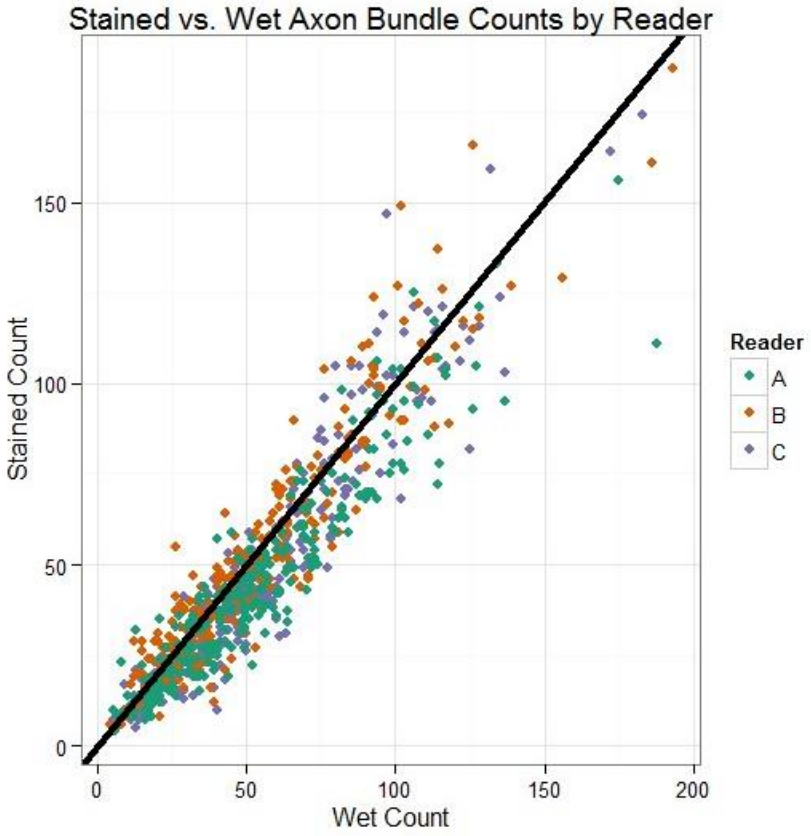


**Figure 4. Graph of stained vs. wet axon counts.** Graph depicting differences in a reader's (A, B, or C) stained and wet axon bundle counts. The trendline (45$^{o}$ angle) represents were points would fall if wet and stained counts for a bundle were the same. Because more points fall below the trendline, the graph indicates that wet counts tend to be higher than stained counts.

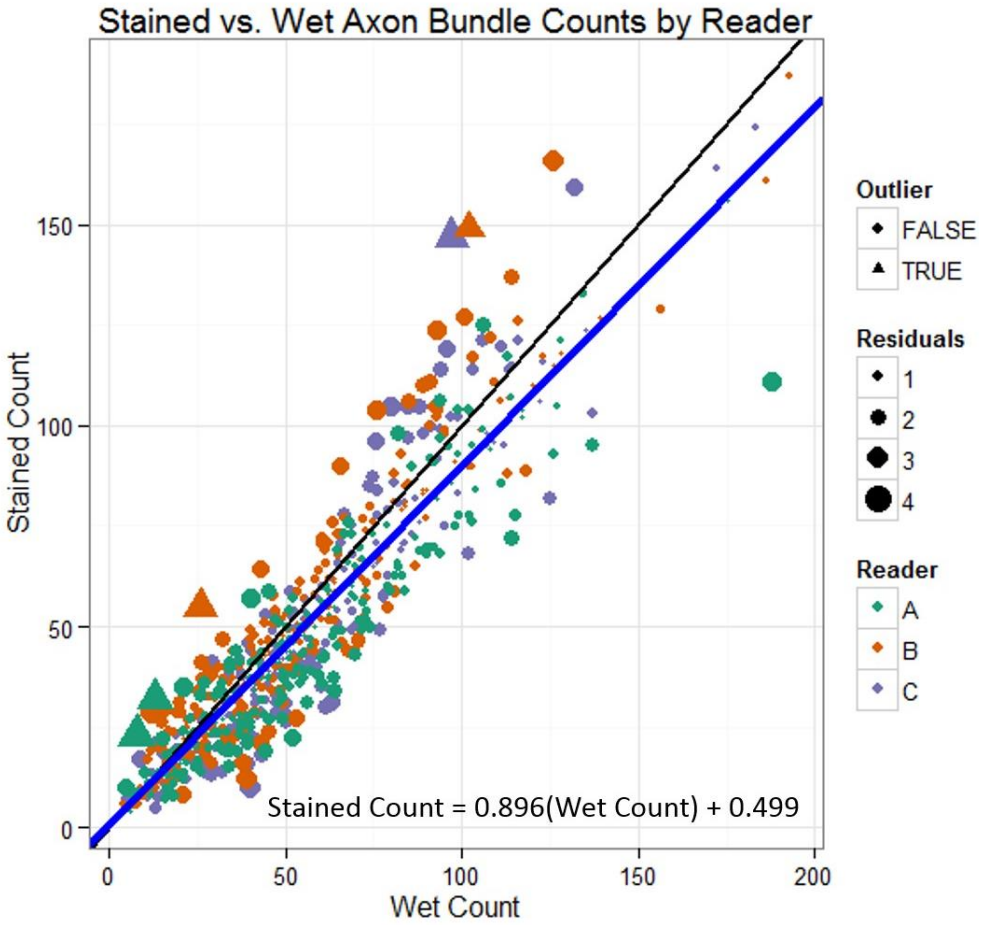


**Figure 5. Linear mixed-effects model for stained vs. wet axon counts.** Linear mixed-effects model plotted as a blue trendline (black trendline is 45º). Smaller residuals are represented by decreasing point sizes, and outliers (residuals>3.5) are plotted as triangles. The model equation is shown on the plot and suggests that, on average, readers counted 10.4% more axons when analyzing wet-mounted, unstained bundles.

Standard deviations and averages were also obtained for the two techniques. The average standard deviation among the readers for wet bundles was 4.29 (max=27.05, min=0), but increased to 5.61 (max=33.26, min=0) for stained bundles. The average standard deviation between the two methods was 2.67 (max=21.74, min=0). Only seven bundles maintained the same standard deviation by all readers before and after staining.

Overall means for wet-counted bundles were 50.7, 51.7, and 52.0 (n=412), while stained-counted bundle means were lower and more variable: 43.8, 46.7, and 49.7 (n=278).

From these statistical analyses, and after considering the quantity of cross-sections or axon bundles that were lost or rendered unusable due to capricious staining, we are confident in reporting that counting axons sans staining is undeniably reliable and more efficient. Readers counting from unstained, wet-mounted axon bundles had higher inter-reader reliability, lower standard deviation, and closer overall means. In addition, we propose this sans-staining technique is also more accurate. Due to the staining process and/or ethanol exposure during the dehydration process, axon bundles markedly shrink, thereby rendering them less discernible and more likely to be under-represented (Figure 6). Consequently, only wet-mounted, unstained data were analyzed in this study, and we suggest only quantifying axon counts from unstained sections in the future.

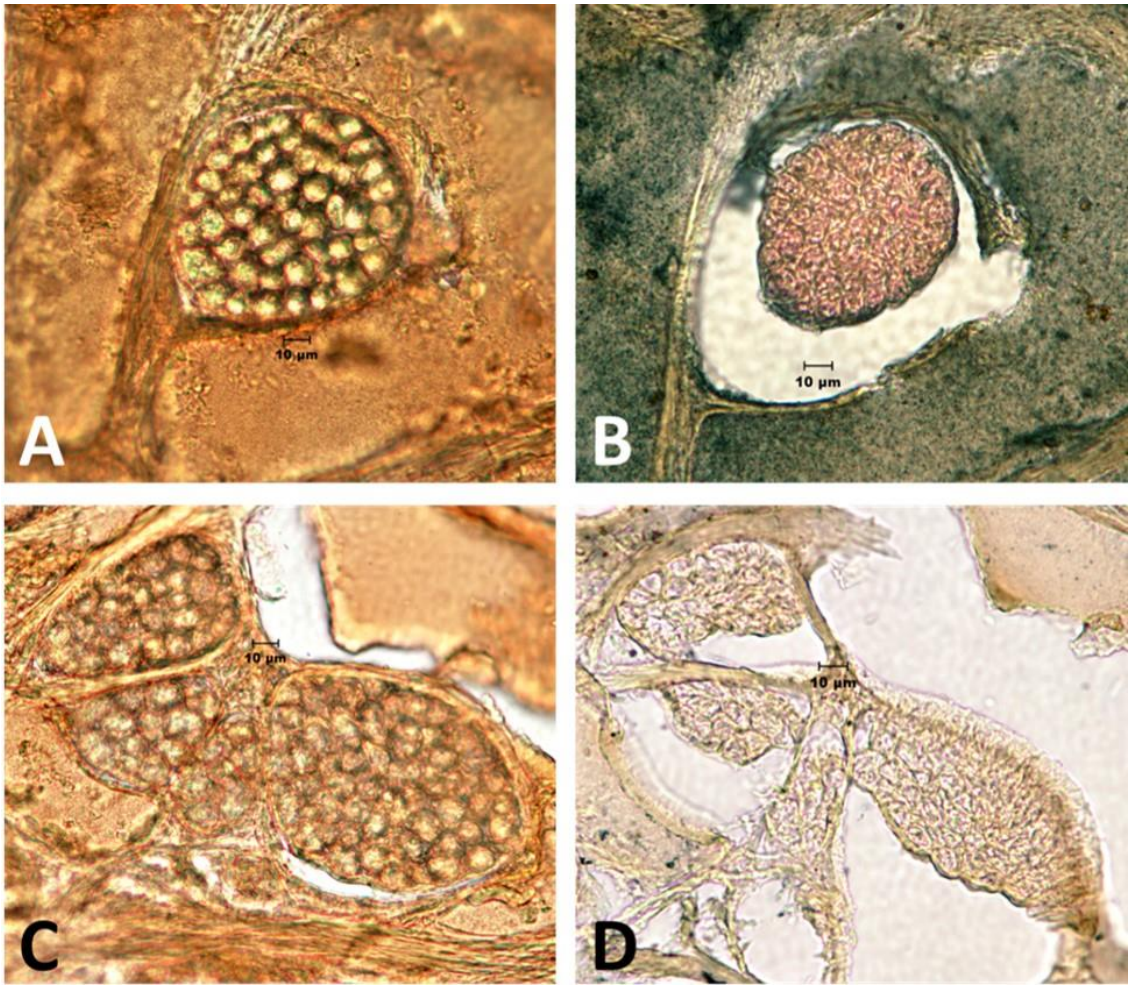


**Figure 6. Axon bundles before (A,C) and after (B,D) staining.** A) Image of an unstained, wet axon bundle. B) Image A axon bundle after staining. Similarly, images C and D show axons before and after staining, respectively. Image B is close to an ideal stain, whereas axons shown in image D stained light and cluster tightly together, making quantification more difficult. Note the substantial axon bundle shrinking during the staining process. Scale bar is 10µm.

## 2.6 *Innervation and Axon Density Analyses*

R was used for all innervation and axon density statistical analyses. The 24 cross-sections measured for morphometrics were matched to their corresponding axon count. The relationship between axon count and F-SC surface area (excluding DC and HS area)

was analyzed using a generalized non-linear least squares model. The data met normality assumptions (affirmed with Cook's distance, a Quantile-Quantile plot, and a Shapiro-Wilk test). Because minor heteroscedasticity in variance existed, the *varPower* function in R was used to replace the homoscedasticity assumption of the least squares model. This model had the best AICc value and diagnostic plots strongly supported its use.

Axon counts divided by F-SC surface area (excluding DC and HS area) yielded axon densities. A linear regression model was used to analyze axon density vs. vibrissa column position on the mystacial vibrissal array. The data met the normality standards for the aforementioned tests and showed reasonably constant variance along the regression line. Results for all analyses were considered significant if the p-value$<0.05$.

# 3. RESULTS

## 3.1 *Mystacial Vibrissal Array*

The range per pad was 43-55 vibrissae, with a mean of 48.0 ± 3.66, indicating an overall average of 96.0 vibrissae per muzzle. The greatest vibrissal pad span (width and length) was 41.6mm ± 2.52mm and 33.5mm ± 3.27mm, respectively. Vibrissae were organized into 6-8 rows (mean=7.0 ± 0.71) and 10-11 columns (mean: 10.2 ± 0.45). Overall, HS length decreased from lateral to medial vibrissae and ranged from 106.2mm to 12.2mm (n=69; Table 1). Both lateral and medial HSs had discernable beading (Figure 7). No noticeable abrasions were present on the muzzle or vibrissae, but it is possible that the true lengths of the HSs were slightly longer at one point in time.


**Figure 7. Beaded hair shaft profile of medial harp seal vibrissae.** Image highlighting the beaded structure along a column 1 (top) and a column 2 (bottom) HS. Scale bar equals 1mm.

**Table 1. Vibrissae hair shaft lengths across the muzzle (n=69).**

| Vibrissa Column | Mean (mm) | S.D. | Minimum HS (mm) | Maximum HS (mm) | n= |
|---|---|---|---|---|---|
| 1 (Medial) | 16.4 | 5.56 | 12.2 | 22.7 | 3 |
| 2 | 21.1 | 6.00 | 16.1 | 27.8 | 3 |
| 3 | 26.0 | 4.23 | 20.5 | 32.1 | 6 |
| 4 | 36.9 | 0.43 | 36.6 | 37.2 | 2 |
| 5 | 35.9 | 8.47 | 25.1 | 44.6 | 4 |
| 6 | 48.6 | 12.54 | 23.3 | 56.9 | 6 |
| 7 | 58.2 | 14.59 | 34.3 | 69.8 | 5 |
| 8 | 61.1 | 16.61 | 33.1 | 84.7 | 12 |
| 9 | 72.7 | 14.52 | 45.7 | 106.2 | 15 |
| 10 | 91.8 | 9.88 | 76.0 | 103.0 | 12 |
| 11 (Lateral) | 81.8 | NA | NA | NA | 1 |

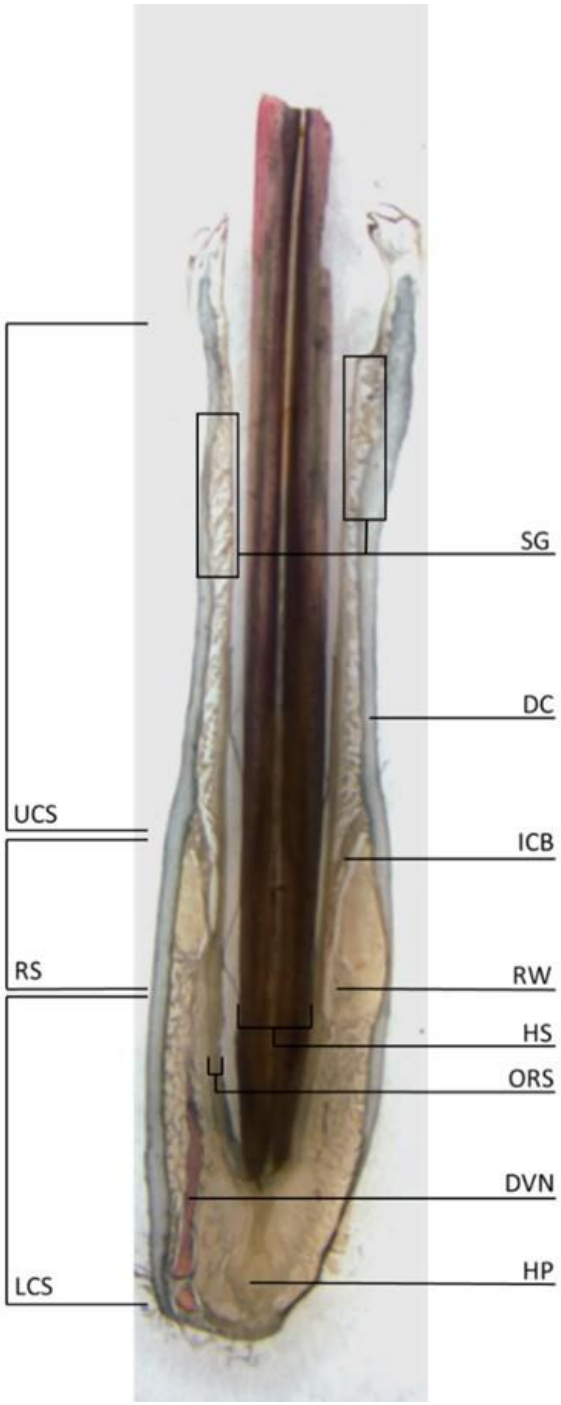


**Figure 8. Silver-stained longitudinal section**. Image depicts the tripartite blood sinus system (i.e., UCS, RS, LCS), the DVN, and other major structures. SG is showing the general location of sebaceous glands within the UCS (1X magnification).

### 3.2 *F-SC Microstructure*

The general microstructure and pattern of innervation in medial and lateral F-SCs were the same. A LCS, RS, and UCS were present in all F-SCs, forming a tripartite blood sinus system within the F-SC (Figure 8). In medial and lateral F-SCs, the UCS comprised ~57% and ~59% of the total F-SC sinus length, respectively. The RS made up ~21% of the total F-SC sinus length in medial vibrissae and constituted ~18% of the sinus length in lateral vibrissae. The LCS was ~27% and ~31% of the total F-SC sinus length in medial and lateral vibrissae, respectively (Tables 2 and 3). The standard deviations on these percentages were large enough to make the differences between medial and lateral F-SC proportions negligible. For both medial and lateral F-SCs, we measured the ratio of asymmetry between RS sides within each F-SC by dividing the maximum RS lengths on both sides of the F-SC from longitudinal sections (Tables 2 and 3). Ratios indicated that lateral F-SCs have more asymmetrical RSs than medial F-SCs. Lateral F-SC RSs had a ratio of 0.7 ± 0.12, whereas medial F-SC RSs had an increased ratio of 0.8 ± 0.08 (1.00 would be perfect symmetry). The maximum RS ratio, 0.9, was the same for both medial and lateral F-SCs. However, the minimum ratios were 0.5 and 0.7 for lateral and medial F-SCs, respectively.

**Table 2. Longitudinal morphometric measurements for large, lateral vibrissae (n=16).**

| | Mean | S.D. | Minimum | Maximum |
|---|---|---|---|---|
| Max F-SC Length (mm) | 12.7 | 1.46 | 10.8 | 16.5 |
| Max Length UCS (mm) | 7.1 | 1.33 | 4.4 | 9.9 |
| Max Length RS (mm) | 2.2 | 0.29 | 1.6 | 3.0 |
| Ratio of the Max Lengths of both RSs in the F-SC | 0.7 | 0.12 | 0.5 | 0.9 |
| Max RS Width (mm) | 0.6 | 0.08 | 0.5 | 0.8 |
| Max Length LCS (mm) | 3.7 | 0.57 | 3.1 | 5.2 |
| Total Sinus Length (mm) | 12.0 | 1.73 | 9.2 | 16.4 |
| % UCS Length to Total F-SC Sinus Length (mm) | 59.2 | 4.19 | 47.5 | 65.1 |
| % RS Length to total F-SC Sinus Length (mm) | 18.1 | 2.41 | 13.3 | 23.9 |
| % LCS Length to total F-SC Sinus Length (mm) | 31.1 | 3.03 | 26.6 | 39.1 |

**Table 3. Longitudinal morphometric measurements for small, medial vibrissae (one column 2 vibrissa, two column 3 vibrissae, n=3).**

| | Mean | S.D. | Minimum | Maximum |
|---|---|---|---|---|
| Max F-SC Length (mm) | 6.8 | 0.90 | 6.1 | 8.0 |
| Max Length UCS (mm) | 3.4 | 0.80 | 2.8 | 4.5 |
| Max Length RS (mm) | 1.3 | 0.09 | 1.1 | 1.4 |
| Ratio of the Max Lengths of both RSs in the F-SC | 0.8 | 0.08 | 0.7 | 0.9 |
| Max RS Width (mm) | 0.5 | 0.06 | 0.4 | 0.6 |
| Max Length LCS (mm) | 1.6 | 0.29 | 1.2 | 1.9 |
| Total Sinus Length (mm) | 6.0 | 1.00 | 4.9 | 7.3 |
| % UCS Length to total F-SC Sinus Length (mm) | 56.9 | 5.92 | 47.2 | 62.3 |
| % RS Length to total F-SC Sinus Length (mm) | 21.3 | 3.52 | 15.8 | 24.0 |
| % LCS Length to total F-SC Sinus Length (mm) | 27.1 | 4.31 | 23.1 | 33.0 |

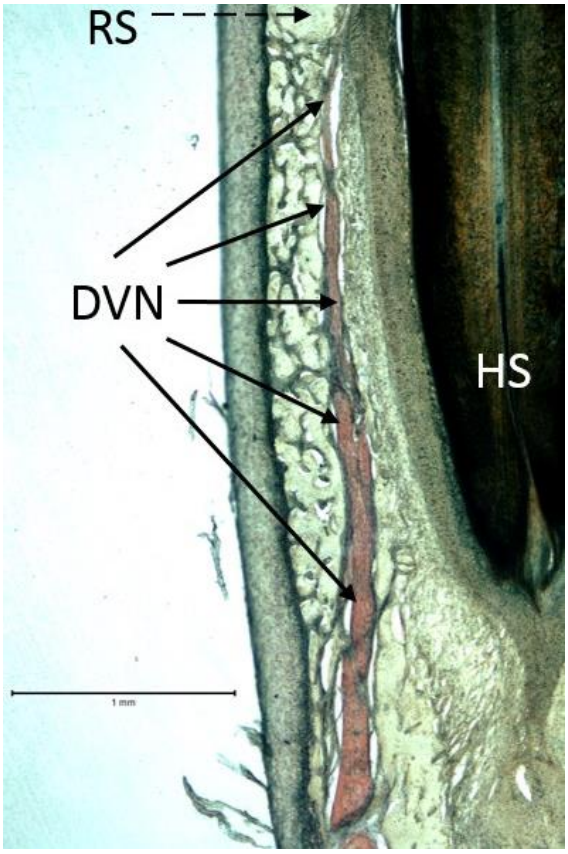


**Figure 9. Close-up of the deep vibrissal nerve.** Silver-stained, longitudinal section highlighting the progression of the DVN through the LCS. Scale bar equals 1mm.

The DVN penetrated the DC of all F-SCs at the base and diminished in size after mid-LCS as it progressed apically towards the RS (Figure 9). After innervating structures in the RS, any remaining branches of the DVN terminated at the ICB. No evidence of a superficial vibrissal nerve was observed in any vibrissal UCSs. The GM, which was most pronounced at the base of the RS, also ended at the ICB (Figure 10). Throughout the LCS and RS, the GM laterally bordered the ORS, and presumptive mechanoreceptors were located at the GM and ORS interface (Figures 10 and 11). Mechanoreceptors that were observed at this interface throughout the LCS, RS, and ICB were presumed to be MNCs. Presumptive lanceolate endings appeared to be located more in the basal RS area. While the GM terminated at the ICB, the ORS continued throughout the UCS. For the entire length of the F-SC, the ORS ran laterally to the IRS, which ran immediately adjacent to the HS and follicle lumen.

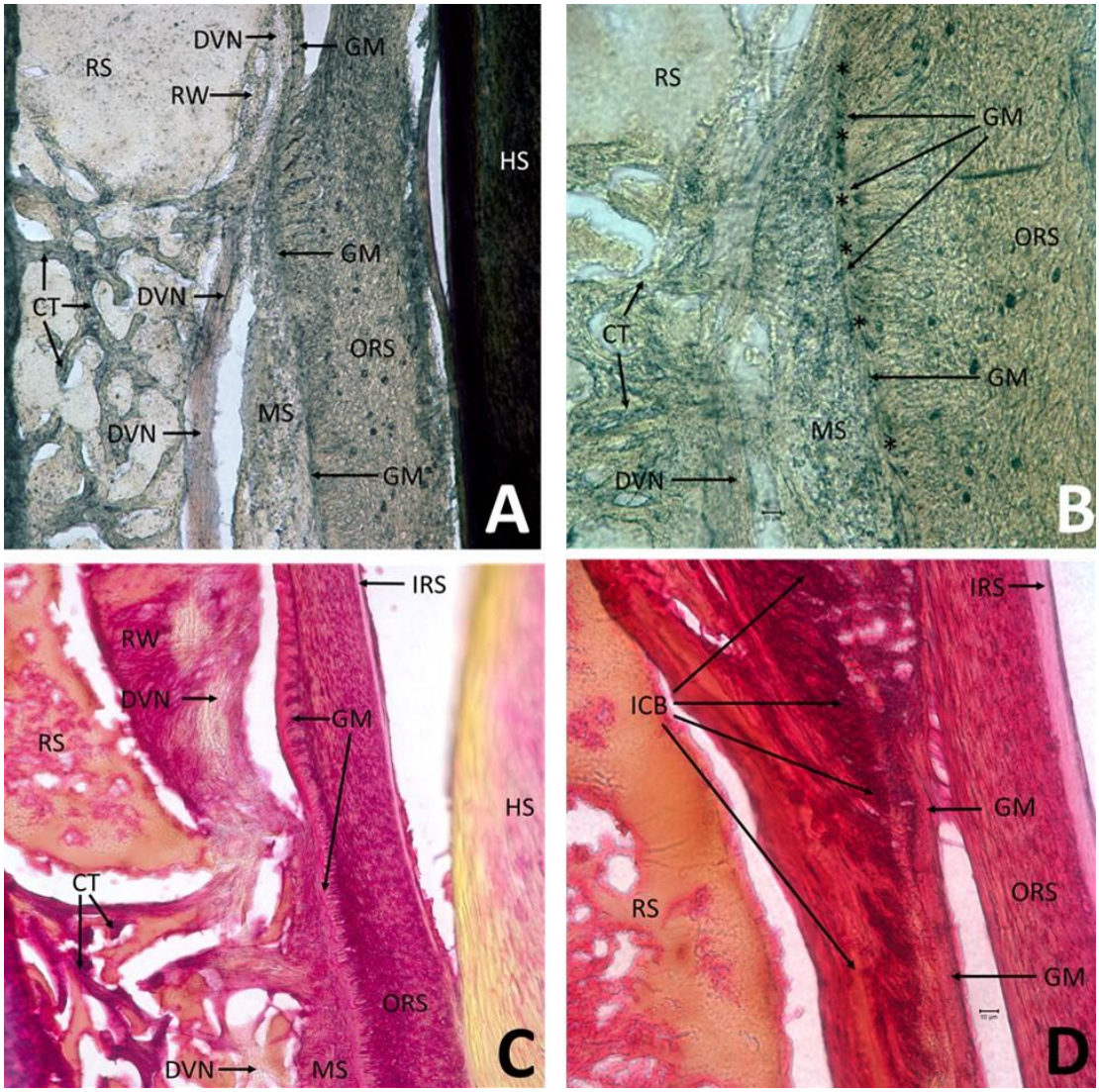


**Figure 10. Close-up of F-SC microanatomical structures.** Images A (20X) and B (40X) are of silver-stained sections from the top of the LCS. Image C (20X) is of a trichrome-stained section from a similar location, whereas image D (40X) is from the top of the RS. Image A shows the course of the DVN and GM through the LCS, RW, and beginning of the RS. The GM enlargement towards the RS base can be seen in B and C. Image B also demarcates the location of presumptive lanceolate endings with asterisks. Image D is a close-up of the ICB and shows the discontinuation of the GM past the ICB. Scale bars for B and D are 10µm.

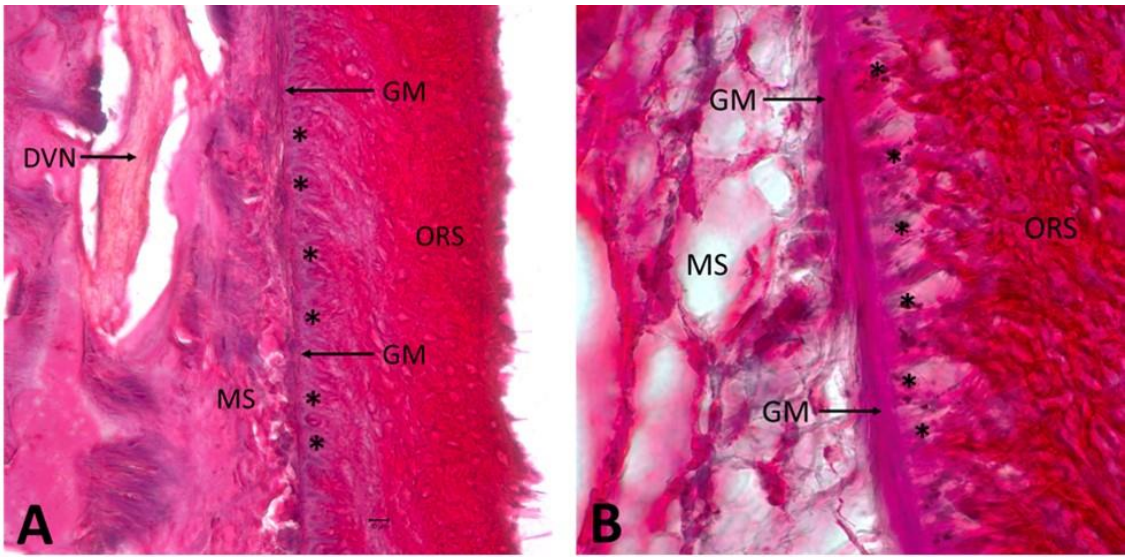


**Figure 11. Presumptive mechanoreceptors.** Images from trichrome-stained portions of the ORS, GM, and MS within the upper LCS. Location of presumptive MNCs are highlighted by asterisks in both A (40x, scale bar=10μm) and B (100X).

All F-SCs possessed CT and MS tissues throughout the UCSs and LCSs, but these tissues were absent in the RS. The MS was observed in the LCS, running laterally alongside the GM. Superficial to the MS, the CT permeated the remainder of the F-SCs to the DC border (Figures 12 and 13). As mentioned previously, asymmetry was seen in the distribution of the RS and RW (Figure 13). Remarkably, despite being roughly half the length of lateral F-SCs, medial F-SCs possessed comparable RS widths. Medial F-SCs had a mean RS width of 0.5 ± 0.06mm. The mean RS width for lateral F-SCs was 0.6 ± 0.08mm, the maximum RS width value for medial F-SCs (Tables 2 and 3).

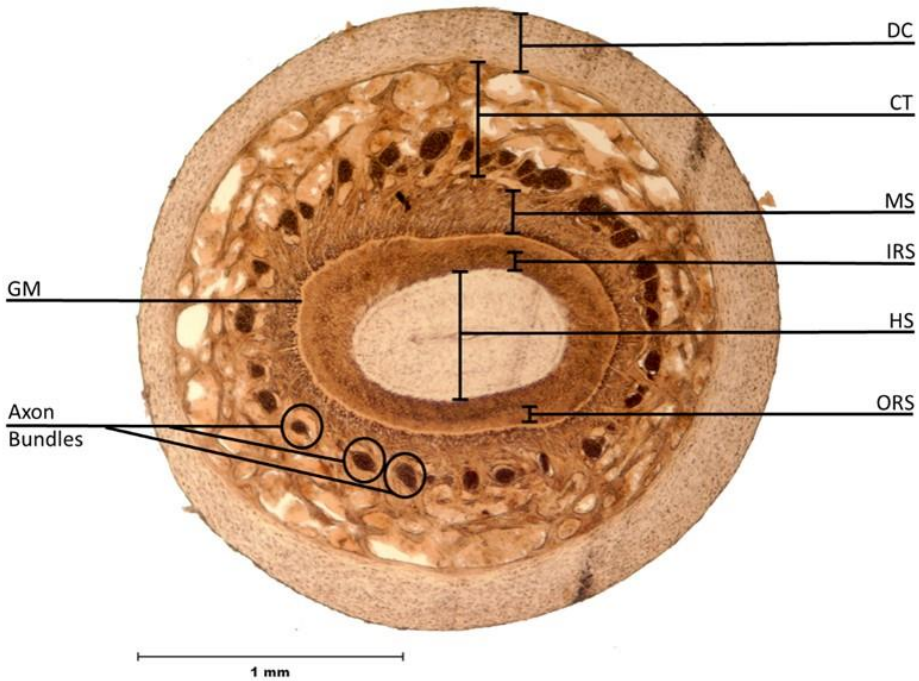


**Figure 12. Unstained cross-section showing microanatomical structures.** An unstained, column 6 vibrissal cross-section showing major aspects of the F-SC.

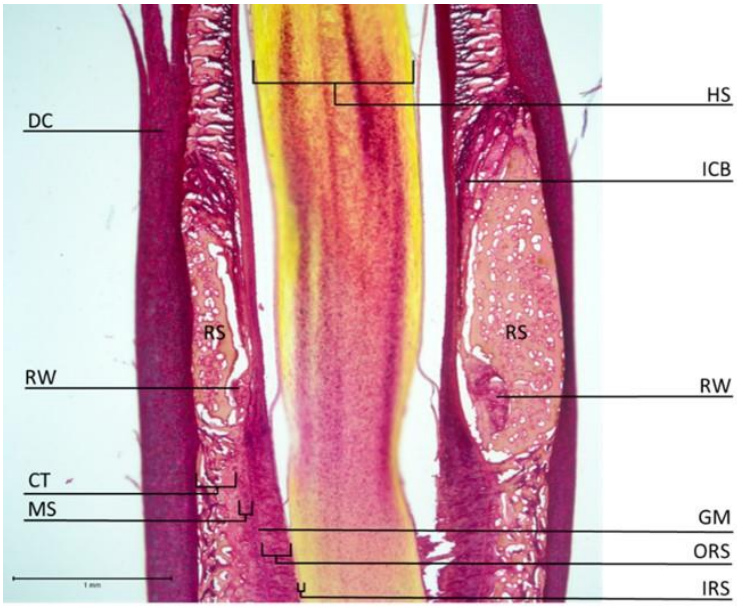


**Figure 13. Magnification of the ring sinus area.** Close-up of a trichrome-stained RS from a lateral F-SC that shows major regions of the F-SC. Note the asymmetry of the RS and RW. Scale bar equals 1mm.

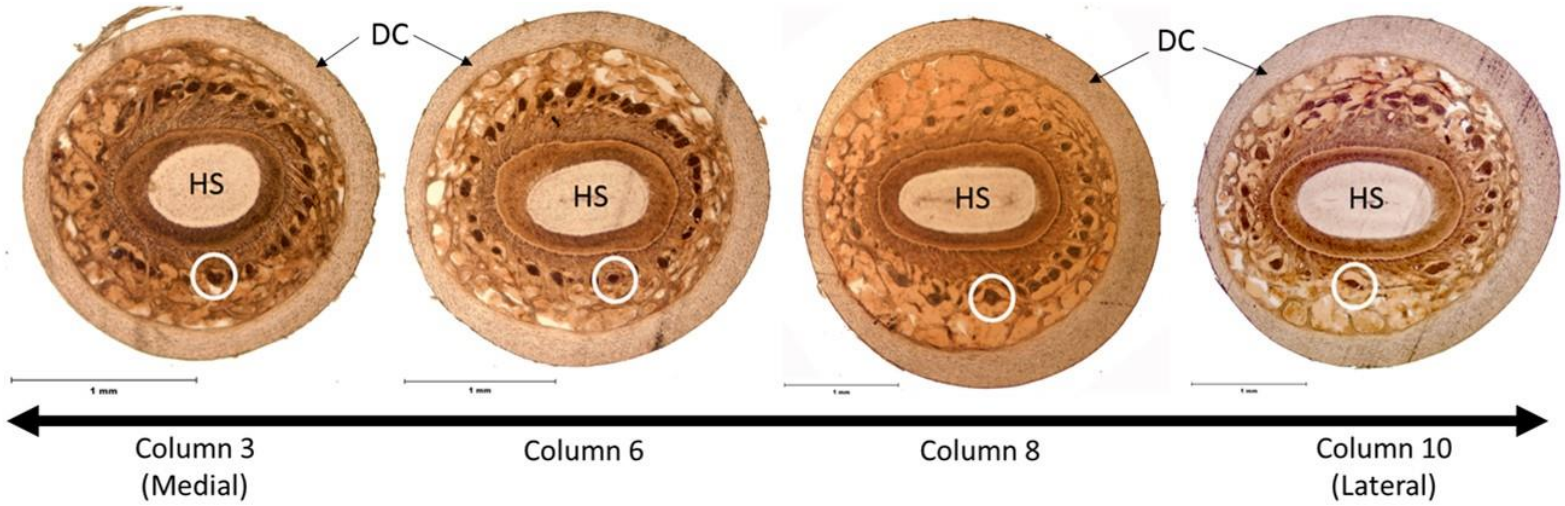


**Figure 14. Cross-sectional microanatomy of F-SCs across the muzzle.** Unstained F-SC cross-sections showing that the DC and axon bundles are more asymmetrical in lateral F-SCs but become more symmetrical in medial F-SCs. White circles demarcate an axon bundle to show their general location within the F-SC. Also note how the HS is more circular in more medial F-SCs. All four cross-sections are from the same harp seal and are considered representative. Scale bars equal 1mm.

All F-SCs were encased in a DC layer of varying thicknesses. Measurements from cross-sections showed a distinctly asymmetrical DC distribution in more laterally located F-SCs, but this asymmetry decreased as F-SCs became progressively more medial (Figure 14). Interestingly, the thinnest DC measurements remained relatively constant despite increases in F-SC size. The mean thinnest DC width of column 1 F-SCs was 0.10mm ± 0.098mm, while column 3, 5, 10, and 11 F-SCs all yielded 0.09mm as their mean thinnest DC width (Table 4). Across all vibrissal columns, the mean thinnest DC width was 0.1mm with a standard deviation of only 0.03mm (n=23). Moreover, medial F-SCs maintained a relatively consistent DC thickness throughout the LCS (Figure 15). Conversely, lateral F-SCs showed a drastic DC thinning at the extreme basal end of the F-SC that comparatively diminished as the DC progressed to the RS (Figure 16).

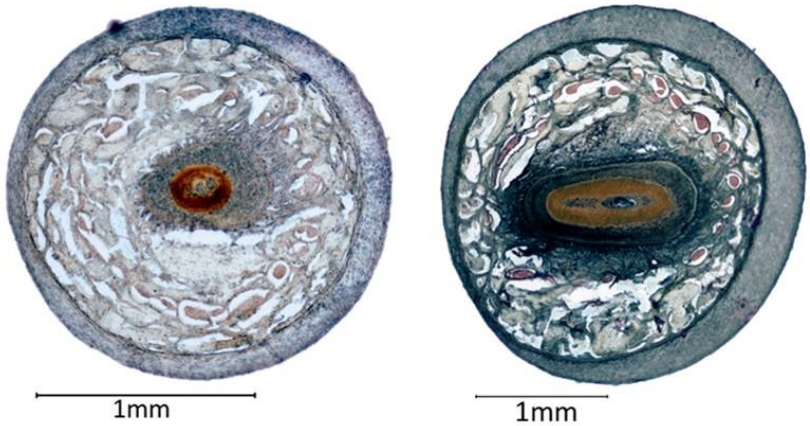


**Figure 15. Silver-stained cross-sections near F-SC base.** Images of a silver-stained medial, column 3 F-SC (left, dyed light) and a lateral, column 10 (right) F-SC that compare F-SC microstructure at the extreme basal end of the F-SC. Note the differences in DC thickness and the shape of the HS.

**Table 4. Summary of cross-sectional morphometrics across the muzzle (n=23).**

| Vibrissa Column Position on Muzzle | 1 (Medial) | 2 | 3 | 5 | 6 | 8 | 9 | 10 | 11 (Lateral) |
|---|---|---|---|---|---|---|---|---|---|
| Mean Max Diameter (mm) | 1.62 ± 0.113 | 1.60 | 1.88 ± 0.129 | 2.24 ± 0.104 | 2.43 ± 0.033 | 2.97 ± 0.307 | 3.19 ± 0.233 | 3.14 ± 0.150 | 3.22 |
| Mean Ratio HS Diameters (mm) | 1.23 ± 0.182 | 1.25 | 1.49 ± 0.232 | 1.63 ± 0.119 | 1.67 ± 0.193 | 1.99 ± 0.304 | 2.01 ± 0.061 | 1.73 ± 0.262 | 2.12 |
| Mean Thinnest DC (mm) | 0.10 ± 0.098 | 0.05 | 0.09 ± 0.024 | 0.09 ± 0.019 | 0.13 ± 0.009 | 0.13 ± 0.019 | 0.12 ± 0.035 | 0.09 ± 0.039 | 0.09 |
| Mean Thickest DC (mm) | 0.19 ± 0.022 | 0.13 | 0.18 ± 0.024 | 0.23 ± 0.038 | 0.31 ± 0.056 | 0.38 ± 0.019 | 0.41 ± 0.031 | 0.42 ± 0.098 | 0.53 |
| Mean DC (mm) | 0.14 ± 0.005 | 0.09 | 0.14 ± 0.016 | 0.16 ± 0.023 | 0.22 ± 0.033 | 0.26 ± 0.011 | 0.26 ± 0.013 | 0.27 ± 0.062 | 0.33 |
| Mean Thinnest MS (mm) | 0.03 ± 0.013 | 0.03 | 0.10 ± 0.087 | 0.13 ± 0.079 | 0.07 ± 0.017 | 0.07 ± 0.021 | 0.08 ± 0.015 | 0.14 ± 0.123 | 0.05 |
| Mean Thickest MS (mm) | 0.14 ± 0.033 | 0.14 | 0.24 ± 0.115 | 0.31 ± 0.048 | 0.23 ± 0.066 | 0.31 ± 0.002 | 0.33 ± 0.047 | 0.34 ± 0.116 | 0.28 |
| Mean MS (mm) | 0.08 ± 0.011 | 0.08 | 0.17 ± 0.104 | 0.21 ± 0.058 | 0.14 ± 0.030 | 0.18 ± 0.007 | 0.18 ± 0.001 | 0.23 ± 0.130 | 0.15 |
| Mean Thinnest CT (mm) | 0.20 ± 0.019 | 0.02 | 0.17 ± 0.084 | 0.19 ± 0.106 | 0.23 ± 0.025 | 0.30 ± 0.050 | 0.27 ± 0.010 | 0.22 ± 0.090 | 0.05 |
| Mean Thickest CT (mm) | 0.34 ± 0.018 | 0.28 | 0.30 ± 0.109 | 0.38 ± 0.106 | 0.42 ± 0.019 | 0.54 ± 0.157 | 0.56 ± 0.051 | 0.49 ± 0.101 | 0.60 |
| Mean CT (mm) | 0.26 ± 0.014 | 0.18 | 0.23 ± 0.096 | 0.28 ± 0.108 | 0.32 ± 0.016 | 0.42 ± 0.094 | 0.42 ± 0.011 | 0.35 ± 0.098 | 0.36 |
| Mean Angle Thinnest DC with Midline (degrees) | 46.7 ± 47.01 | 19.9 | 35.9 ± 18.59 | 15.0 ± 10.54 | 7.4 ± 2.79 | 5.7 ± 3.38 | 9.1 ± 7.90 | 14.9 ± 15.46 | 30.5 |
| Mean Angle Thinnest DC with Thickest DC (degrees) | 60.0 ± 14.88 | 5.2 | 36.7 ± 14.67 | 42.0 ± 12.16 | 57.0 ± 25.92 | 60.8 ± 24.68 | 57.8 ± 34.22 | 40.4 ± 30.03 | 19.5 |
| Number of Cross-sections Analyzed | 2 | 1 | 4 | 4 | 3 | 2 | 2 | 4 | 1 |

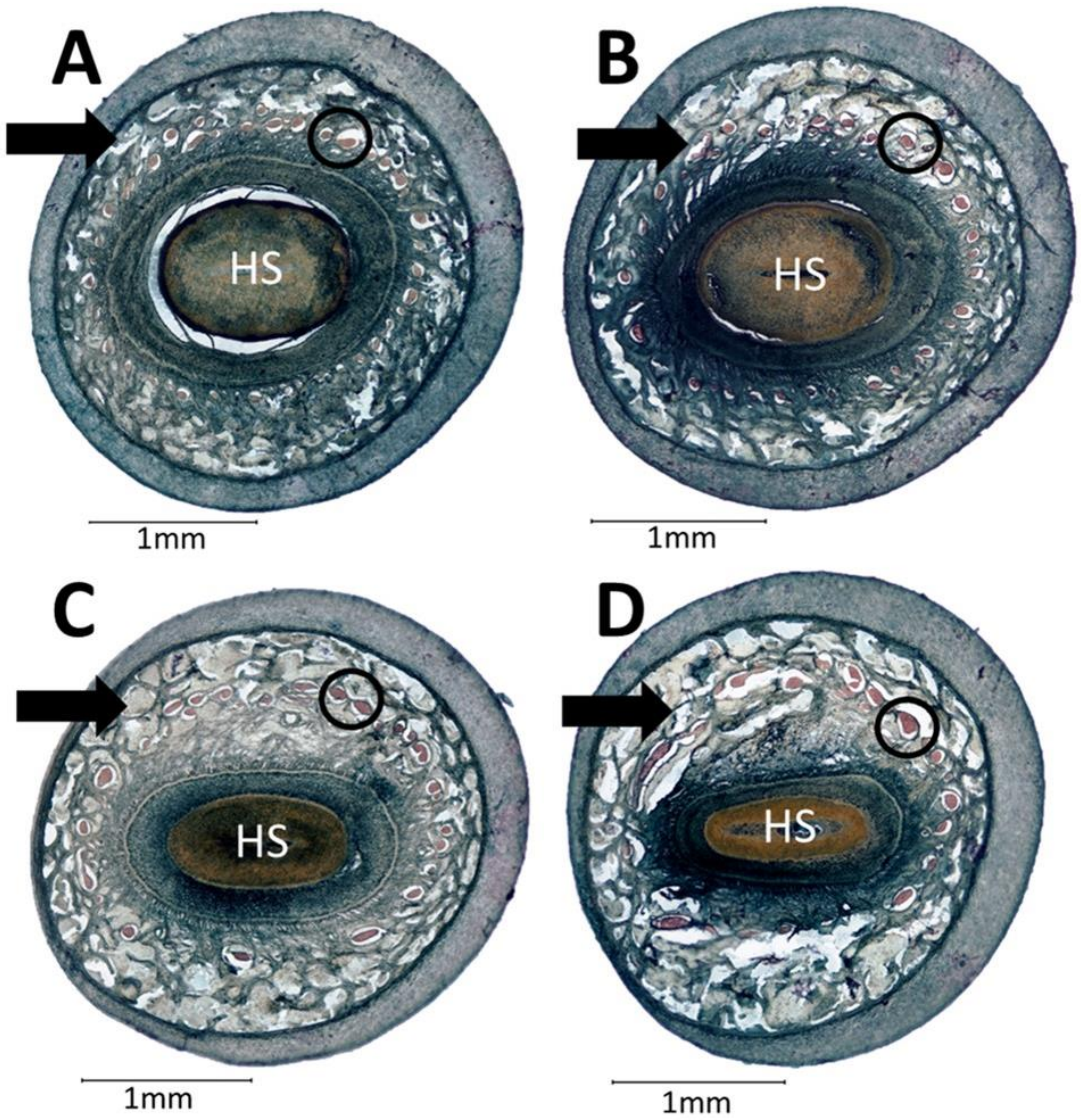


**Figure 16. Vertical progression through a large, lateral F-SC.** Silver-stained, LCS cross-sections from a column 10 F-SC showing morphological differences as sections become more distal from the RS. A) Section just below the RS. B) Several sections below image A. C) Approximately mid-LCS and representative of where axons were quantified. D) Section close to the base of the F-SC. Axon bundles are dyed reddish-brown and example bundles are encircled. Arrows highlight the side of F-SC with denser axon bundles. Note that DC thickness and axon bundle distribution become slightly less asymmetrical as sections progress apically. In addition, the HS becomes more circular towards the RS.

Similar to asymmetries seen in DC thicknesses, major branches of the DVN were more asymmetrically distributed around the HS in lateral F-SCs but became more symmetrically distributed in medial F-SCs (Figure 14). Axon bundles in lateral F-SCs remained asymmetrical throughout the entire span of the LCS (Figure 16). To determine the orientation of axon bundle asymmetries within the muzzle, we purposely added a fiducial mark to two F-SCs from two individuals on their ventral side during dissection (Figure 17). One vibrissa was a left vibrissal pad, row A, column 5 F-SC, while the other was a right vibrissal pad, row B, column 7 F-SC. Despite the variations in row and column position, the results for both F-SCs showed that larger groupings of axons were distributed dorsally. We repeated this process on two additional F-SCs to determine DC thickness orientation. A left pad, row B, column 7 F-SC and a right pad, row A, column 8 F-SC from two individuals were marked either medially or laterally. Again, despite position differences, both F-SCs indicated that thinner DC areas were medial.

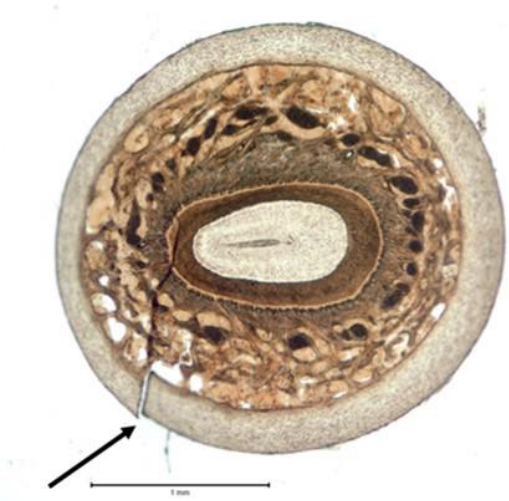

**Figure 17. Fiducial mark in F-SC.** Image depicting the ventral cut on a left vibrissal pad, row A, column 5 F-SC cross-section. More axon bundles are noticeably present dorsally. Scale bar equals 1 mm.

Several F-SCs possessed a dimple (Figure 18). However, dimples were only found on one individual and almost exclusively on the right vibrissal pad. All observed F-SCs within row B of this pad were dimpled in the same location, but a systematic evaluation of the entire mystacial pad was not conducted. We presumed the indentation was an artifact. By personal observation, and by adding fiducial marks to the F-SC as outlined above, we were able to determine that F-SC dimples were always medially located. This information, coupled with longitudinal images of dimpled F-SCs, allowed us to determine that the larger, asymmetrical RSs and RWs sides were located medially.

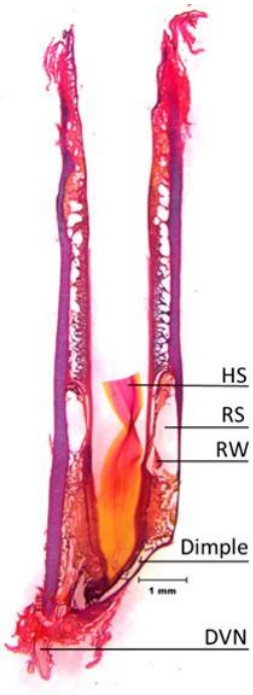


**Figure 18. Trichrome-stained longitudinal section from a dimpled F-SC (compare to Figure 8).** Note the medially located dimple, which indicates that the larger RS and RW areas are also located medially. The HS was cut to facilitate cover-slipping. Scale bar equals 1mm.

HSs in lateral F-SCs had a ratio of 2.12 at the mid-LCS and were more elliptical than medial F-SC HSs. Similar measurements from progressively more medial F-SCs showed that HSs became gradually more circular and attained a minimum mean ratio of 1.23 in column 1 F-SCs (Figure 14, Table 4). The mean angle between the thinnest DC location, HS midpoint, and the HS major axis ranged from 5.7$^{o}$ to 46.7$^{o}$. The mean angle between the thinnest DC portion, HS midpoint, and thickest DC location had a similarly expansive range: 5.2$^{o}$ to 60.8$^{o}$ (Table 4). Since the ranges were so broad and standard deviations were so variable, we were not able to detect any conclusive patterns regarding HS orientation and DC thicknesses.

Multiple SGs and ducts were observed in the apical region of the UCS (Figure 19). Ducts emptied directly from the UCS into the follicle lumen. No apocrine sweat glands or other types of glandular tissues were identified in any F-SCs.

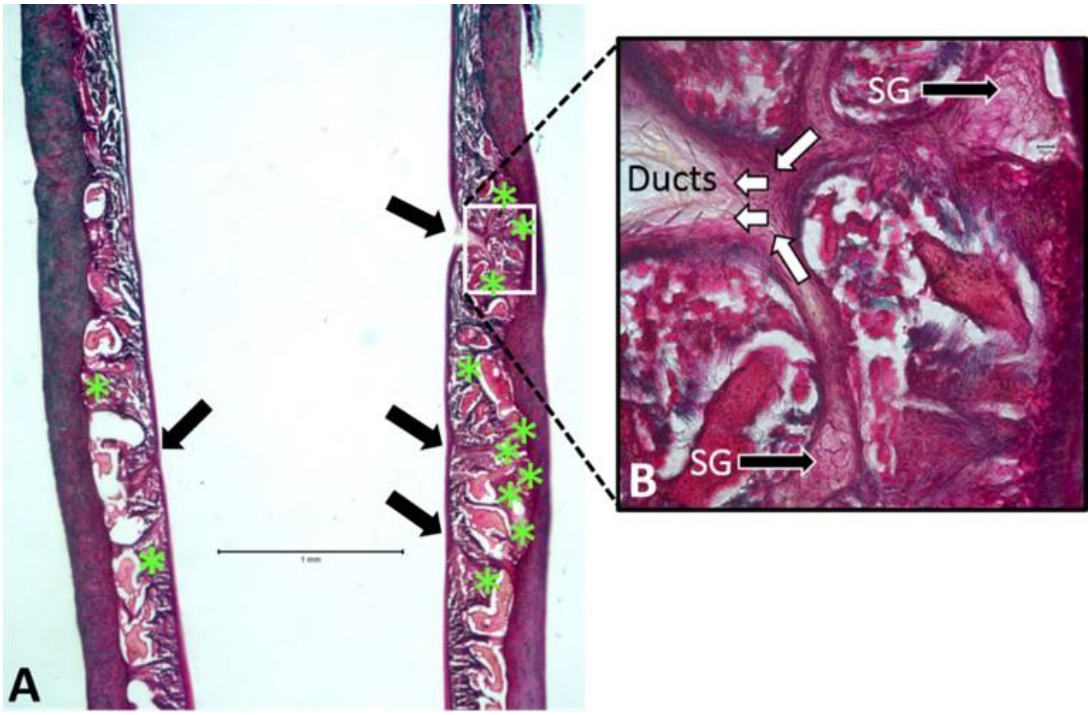


**Figure 19. Sebaceous gland location and microstructure.** A) Image of a trichrome-stained UCS (HS removed). SG locations are demarcated by green asterisks, with visible secretion ducts leading to the follicle lumen highlighted by arrows. Scale bar equals 1mm. B) Magnified SGs (black arrows) and secretion ducts (white arrows). Scale bar equals 10µm.

**Table 5. Axon counts listed by vibrissa column (n=146).** N is the number of cross-sections analyzed.

| Vibrissa Column | Mean Axon Count | S.D. | n= |
|---|---|---|---|
| 1 (Medial) | 550.25 | 97.39 | 4 |
| 2 | 560.13 | 126.7 | 8 |
| 3 | 825.38 | 102.98 | 16 |
| 5 | 1286.42 | 130.48 | 12 |
| 6 | 1357.64 | 191.96 | 14 |
| 7 | 1369.11 | 92.81 | 9 |
| 8 | 1389.3 | 121.29 | 30 |
| 9 | 1624 | 166.54 | 25 |
| 10 | 1632.13 | 173.17 | 23 |
| 11 (Lateral) | 1617.4 | 136.69 | 5 |

### 3.3 *F-SC Innervation*

The mean number of axons innervating large, lateral F-SCs was 1533.6 ± 192.9. This mean extrapolates to an overall mystacial vibrissal array innervation estimate of 147,225.6 (n=82). However, substantial innervation differences existed between medial and lateral F-SCs. Mean medial-to-lateral axon counts ranged from 550.3 ± 97.4 axons/F-SC (column 1) to 1632.1 ± 173.2 axons/F-SC (column 10), respectively (Table 5). Figure 20 shows all axon counts by vibrissa position on the muzzle, with the means plotted as a line graph. Figure 21 depicts mean axon counts by vibrissa position on the muzzle, including some row variations. By including medial estimates, we concluded that a more accurate total of 117,235.2 axons innervate the entire mystacial array.

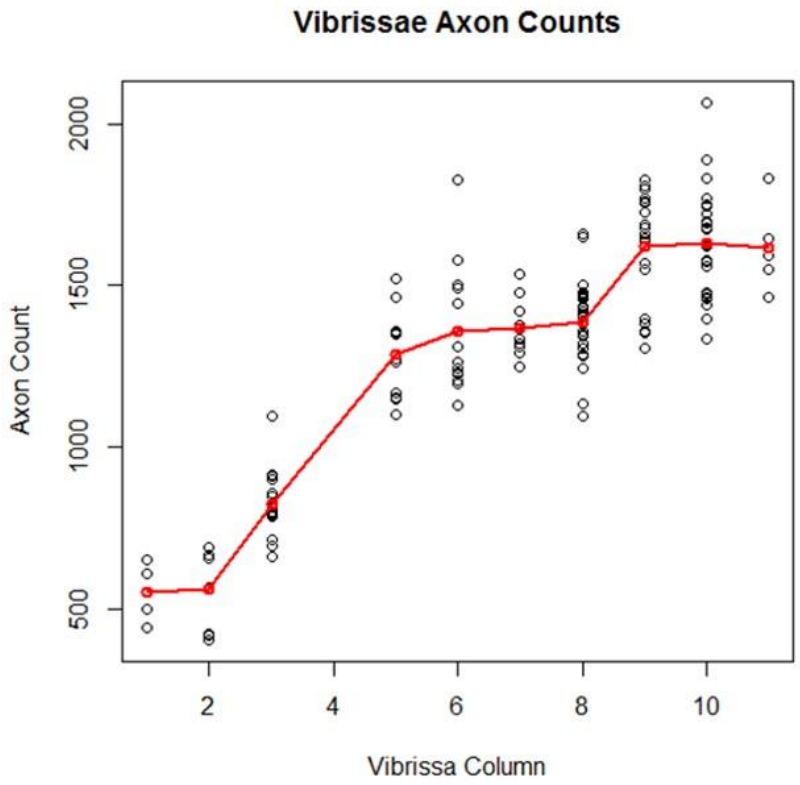


**Figure 20. Graph of axon count (n=146) by vibrissa column (column 1 is medial).** The means for each column are plotted in red and connected with a line graph.

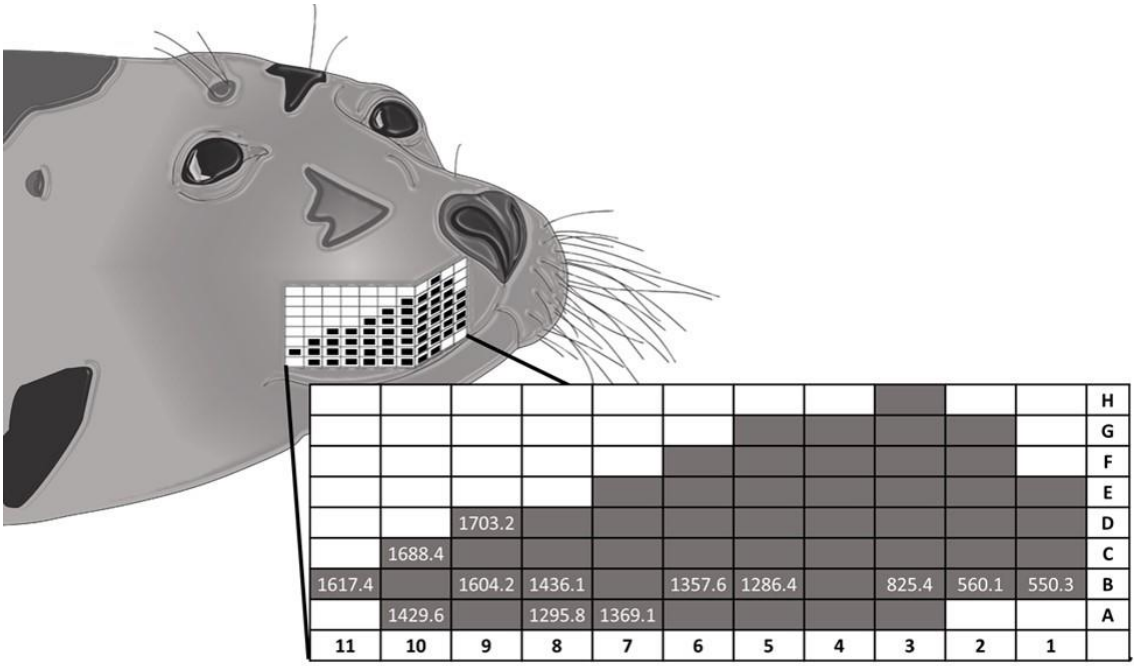


**Figure 21. Vibrissal map showing mean axon counts across the muzzle** (column 1:n=4, column 2:n=8, column 3:n=16, column 5:n=12, column 6:n=14, column 7:n=9, column 8—row A:n=10; column 8—row B:n=20, column 9—row B:n=20, column 9—row D:n=5, column 10—row A:n=5, column 10—row C:n=18, column 11:n=5; n=number of cross-sections)**.**

Medial-to-lateral axon counts were plotted against F-SC surface area (excluding HS and DC) and yielded a highly significant ($p<<0.01$), non-linear trend (Figure 22). However, when these values were converted to axon densities, no significant trend was found between axon density and vibrissa position ($p=0.17$, adjusted $R^2=0.04$; Figure 23). A column 3 F-SC possessed the maximum axon density of 606.7 axons/mm$^2$, while a column 8 F-SC had the lowest axon density at 297.7 axons/mm$^2$. While these data alone may suggest smaller F-SCs have higher axon densities, the variability within the data prevented us from obtaining significant conclusions about axon density and vibrissa position on the muzzle.

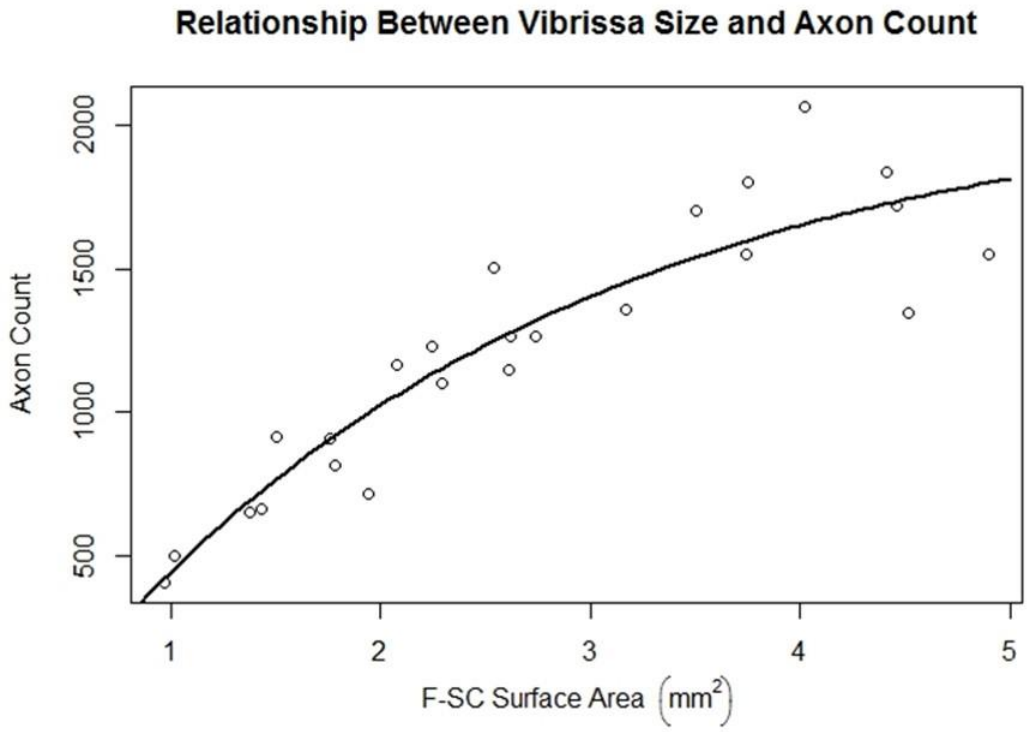


**Figure 22. Graph of F-SC surface area (excluding DC and HS) vs. axon count.**
Trend line plotted using a generalized non-linear least squares model ($p<<0.01$; $n=24$).

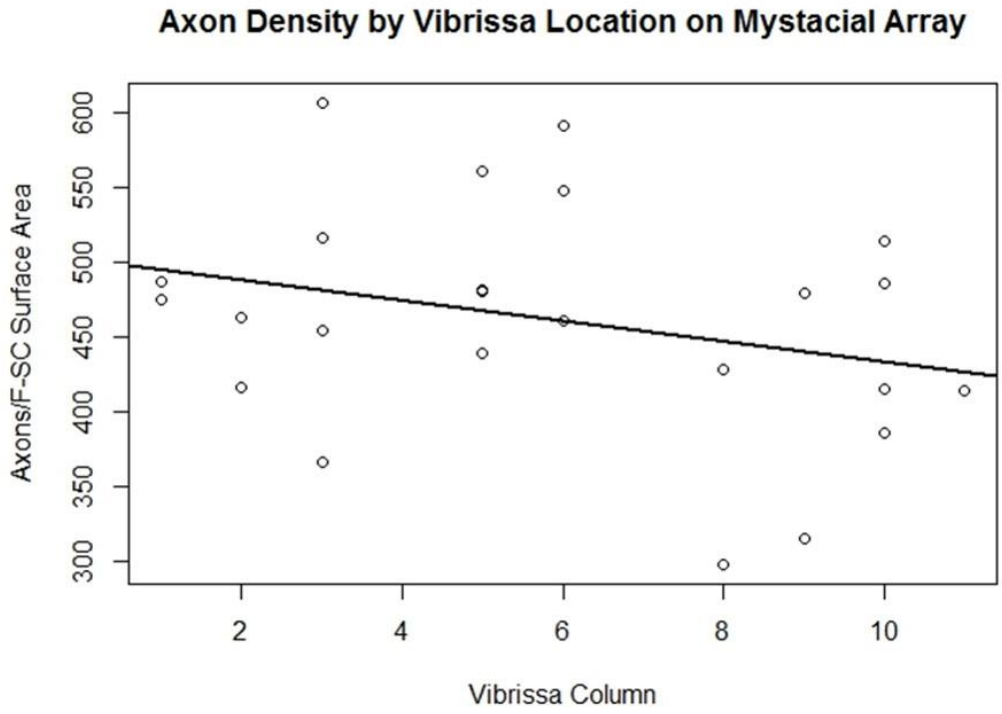


**Figure 23. Graph of axon density vs. vibrissa column (n=24).** Column 1 is medial. Analysis was conducted using a linear regression model ($p=0.17$, adjusted $R^2=0.04$). Surface area was measured in $mm^2$.

# 4. DISCUSSION

## 4.1 *Harp Seal Mystacial Vibrissae*

The number of mystacial vibrissae on our harp seals was comparable to those of other phocids, as well as sea otters and West Indian Florida manatees [Yablokov and Klevezal, 1962; Ling, 1977; Reep et al., 2001; Hyvärinen et al., 2009; Marshall et al., 2014a; McGovern et al., 2015]. The maximum number of mystacial vibrissae per pad (55) was higher than previously reported for harp seals [49; Yablokov and Klevezal, 1962].

Our mean lateral F-SC length was the shortest value reported for multiple pinnipeds [i.e., Ross, ringed, northern elephant (*Mirounga angustirostris*), and bearded seals; Ling, 1972; Marshall et al., 2006; Hyvärinen and Katajisto, 1984; McGovern et al., 2015]. The mean RS percentage to the total sinus length in harp seal F-SCs was similar for both medial and lateral vibrissae (~18-21%). However, this percentage was higher than that reported for northern elephant seal vibrissae [13.9%; McGovern et al., 2015]. Likewise, mean LCS percentages for harp seal vibrissae, both medial and lateral, were similar (~27-31%) but were lower than reported values for northern elephant seal vibrissae [36.6%; McGovern et al., 2015]. The UCS (for both medial and lateral F-SCs) accounted for approximately 60% of the total sinus length, a percentage similar to that found in pinnipeds with larger F-SCs [Marshall et al., 2006; Hyvärinen et al., 2009]. In contrast, this percentage is ~1.5x larger than those seen in northern and southern elephant seals [*Mirounga leonine*; ~40-47%; Ling, 1966; McGovern et al., 2015]. The

UCS, lacking in terrestrial and semi-aquatic mammals, is hypothesized to serve a thermoregulatory function [Lee and Woolsey, 1975; Rice et al., 1986; Marotte et al., 1992; Dehnhardt et al., 1999; Mauck et al., 2000; Hyvärinen et al., 2009; Erdsack et al., 2014]. Harbor seals can selectively heat their vibrissae to keep sensory perception functioning at full capacity despite changes in arctic water temperatures [Mauck et al., 2000; Erdsack et al., 2014]. Harp seals also likely possess this capability, although it has not been directly studied.

The longest harp seal HS (106mm) was shorter than other reported pinniped HS lengths, except those found on Ross seals [40mm; Ling, 1966; 1972; Ladygina et al., 1985; Marshall et al., 2006; McGovern et al., 2015]. HS length regularly decreased as vibrissae became more medial, a pattern evident in other mammals [Brecht et al., 1997]. However, pinnipeds commonly show signs of vibrissal abrasion, which could affect HS length [Fay, 1982; Marshall et al., 2006; McGovern et al., 2015]. Similar to other phocids (excluding monk, leopard, Ross, and bearded seals), harp seal HSs are beaded [Ling, 1972; Berta et al., 2006; Marshall et al., 2006; Ginter et al., 2012]. Harp seal HSs have approximately 1.1 beads/cm but are not known to have beads on vibrissae shorter than ~25mm [Ginter et al., 2010; 2012], which differed from our observations. The predominant hypothesis is that the beads help mitigate unnecessary background water "noise," thereby allowing seals to better cue in on prey wake trails [Hanke et al., 2010; Miersch et al., 2011].

Column 1 HSs were almost completely circular (1.2mm HS diameter ratio), while larger, lateral HSs were unmistakably elliptical (2.1mm HS diameter ratio; Table

4). Moreover, medial vibrissae HSs remained circular throughout the F-SC, but lateral vibrissae HSs appeared to become less elliptical as they neared the RS (Figures 15 and 16). Most pinnipeds have elliptical HSs but exceptions exist [e.g., Ross, Weddell (*Leptonychotes weddellii*); Ling, 1972; Marshall et al., 2006; Hanke et al., 2010; Ginter-Summarell et al., 2015; McGovern et al., 2015]. One study suggests that it is this elliptical aspect of the HS, not the beaded aspect, that aids in dampening background water vortices enough for pinnipeds to distinguish prey trails [Murphy et al., 2013].

HS diameter ratio data indicate that harp seals, and likely pinnipeds in general, have not only a morphological but also a functional difference between their lateral macrovibrissae and their medial microvibrissae. Psychophysical experiments using harbor seals support this hypothesis, but conflicting information on harbor seal vibrissal sensitivities exists, depending on whether seals were exposed to vibrating spheres, rods, or sheets [Renouf, 1979; Mills and Renouf, 1986; Dehnhardt et al., 1998; Murphy et al., 2015]. In-air, tactile experiments that involved harbor seals investigating a vibrating sheet achieved comparable vibrissal sensitivity thresholds as a study that utilized an oscillating sphere underwater [Dehnhardt et al., 1998; Murphy et al., 2015]. However, sensitivity thresholds presented by Murphy *et al.* [2015] were, on average, 100 times lower than similar in-air vibration experiments [Renouf, 1979; Mills and Renouf, 1986]. We suggest that data inconsistencies are the result of differences between micro- and macrovibrissae. In Murphy *et al*.'s [2015] experiment, they used a vibrating sheet and stated that, on average, 14 vibrissae were in contact with the sheet during trials. Murphy *et al.* [2015] attempted to maximize the number of vibrissae in contact with the sheet,

but harbor seals have ~31 vibrissae per mystacial pad [Ling, 1977]. Hence, only approximately half of the vibrissae were being analyzed at any time. Moreover, from Murphy *et al.*'s [2015] figure (Figure 24), it appears that lateral macrovibrissae were primarily in contact with the sheet and smaller, shorter microvibrissae were less likely to contact the sheet.

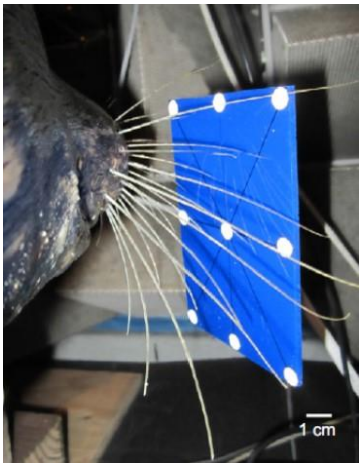


**Figure 24. Position of harbor seal vibrissae during a sensitivity experiment.** Image from Murphy *et al.* [2015][*] showing a stationed harbor seal with its right vibrissal pad contacting the blue, vibrating sheet. The figure shows how vibrissae were positioned during the study and how far away the sheet was from the seal.

Some studies indicate that the elliptical, beaded macrovibrissae that Murphy *et al.* [2015] focused on are best adapted for detecting hydrodynamic water signals because they have optimal sensitivity thresholds for detecting prey wake trails [Bleckmann et al.,

[*] Reprinted with permission from "Vibrissal sensitivity in a harbor seal (*Phoca vitulina*)" by Murphy CT, Reichmuth C, Mann D, 2015. The Journal of Experimental Biology, 218, 2463-2471, Copyright 2015 by The Company of Biologists Ltd.

1991; Dehnhardt et al., 1998; Hanke et al., 2010; Miersch et al., 2011]. We propose that Murphy *et al.*'s [2015] study supports this hypothesis since they mainly analyzed macrovibrissae but obtained results similar to in-water experiments by Dehnhardt *et al.* [1998] that included all vibrissae. In comparison, Mills and Renouf's [1986] and Renouf's [1979] experiments both utilized 6.4mm diameter vibrating rods but neither studies explicitly stated which vibrissae were contacting the rod or how restricted the seal's movement within the apparatus was, thereby making it difficult to make direct comparisons. However, since pinnipeds prefer to localize objects on their medial vibrissae after initial detection with their lateral vibrissae [Kastelein and van Gaalen, 1988; Dehnhardt and Dücker, 1996; Marshall et al., 2008; Grant et al., 2013; Marshall et al., 2014b], it is reasonable to assume that Mills and Renouf's [1986] and Renouf's [1979] harbor seals attempted to preferentially contact the rod with their microvibrissae. More details on the exact experimental design (e.g., which vibrissae were contacting the vibrating object, how much seals could move their head while in the apparatus) from these studies are warranted, but we suggest that discrepancies seen among vibrational studies could be because these studies were not separately analyzing micro- and macrovibrissae. In addition, previous studies asserted that if harbor seals had 1mm diameter, circular HSs, the vortex-induced vibrations from the vibrissae would overlap the functional range of the vibrissal system, thereby making prey capture less effective [Bleckmann et al., 1991; Hanke et al., 2010; Miersch et al., 2011]. Our most medial harp seal HSs were similar in dimension to this theoretical 1mm diameter, circular HS, but our harp seal HSs did not reach a 1mm diameter until they became more lateral, column

6 vibrissae. Consequently, our data support that column 1 F-SCs likely detect vibration frequencies in a different range, apparently one with higher thresholds considering Mills and Renouf's [1986] and Renouf's [1979] analyses. Other researchers have also hypothesized that the pinniped mystacial array is finely tuned, with each vibrissae specialized to perceive different resonances depending its HS morphology [Ginter-Summarell et al., 2015].

Since macrovibrissae appear to be better than microvibrissae at perceiving biologically significant wake frequencies generated by their prey [Bleckmann et al., 1991; Dehnhardt et al., 1998; Hanke et al., 2010; Miersch et al., 2011; Murphy et al., 2015], the higher thresholds detected by microvibrissae appear superfluous. We propose that this information further reinforces the hypothesis that pinniped microvibrissae are instead morphologically designed for object recognition or close-up haptic exploration [Bleckmann et al., 1991; Dehnhardt et al., 1998; Hanke et al., 2010; Miersch et al., 2011; Murphy et al., 2015]. This bipartite vibrissae hypothesis is further supported by the fact that all northern fur seal mystacial vibrissae (except the most dorsal row) project onto the somatosensory cortex as similar sizes [Ladygina et al., 1985]. This indicates that, despite differences in the quantity of innervation, microvibrissae are as functionally important as macrovibrissae, perhaps just tuned for different stimuli.

In essence, we suggest that harp seals rely on their macrovibrissae to initially detect prey wake trails but then capitalize on the close-up, haptic specialization of their microvibrissae during the final stages of prey capture. However, support for this bipartite functional hypothesis in pinnipeds is currently lacking, and the majority of information

obtained from the literature has been inferred. The medial innervation estimate proposed for ringed seals did not include intermediate innervation estimates across the muzzle or specify exactly where on the muzzle vibrissae were sampled [Hyvärinen et al., 2009]. Other published pinniped vibrissal studies either focus on individual vibrissae, macrovibrissae, or the mystacial array as a whole, thereby confounding conclusions about the functional differences between micro- and macrovibrissae. In addition, existing medial-to-lateral innervation and microstructural data for West Indian Florida manatees (fully aquatic herbivores), Australian water rats (semi-aquatic species), and tammar wallabies (*Macropus eugenii*), rats, and mice (terrestrial species) are not comparable to fully aquatic carnivorans [Lee and Woolsey, 1975; Rice et al., 1986; Marotte et al., 1992; Dehnhardt et al., 1999; Reep et al., 2001]. Our presented research on harp seal F-SCs is the first attempt to quantitatively and qualitatively support this bipartite functional hypothesis among pinnipeds by systematically investigating the microanatomical and innervational differences between micro- and macrovibrissae, but it is clear further research is warranted.

### 4.2 *F-SC Microstructure*

Harp seal F-SCs were organized in a tripartite blood sinus system and possessed the same general design, innervation location, and tissues as those of other phocids. Interestingly, the microstructure of macro- vs. microvibrissae were similar particularly in their morphometrics. HS beading and proportions of the LCS, RS, and UCS were similar between vibrissae types. Both macro- and microvibrissae had asymmetrical RSs and

RWs. We also observed that macrovibrissae RSs were more asymmetrical than microvibrissae RSs (Tables 2 and 3), which could stem from macrovibrissae perhaps being more directionally sensitive. Notably, despite size differences, both types of vibrissae had similar RS widths. The asymmetrical RW is thought to help regulate blood flow and/or relay vibration signals from the HS into the RS [Ling, 1966; Stephens et al., 1973]. Interestingly, despite their substantially larger overall size, southern elephant seal F-SCs have a comparatively small RW when compared to that of mice [Ling, 1966].

Two important F-SC attributes were noted that could contribute to differences in vibrissal sensitivity and support the need to differentiate between macro- and microvibrissae in pinnipeds. These were DC thickness and axon bundle distribution. Our harp seal DCs had distinctly thinner and thicker portions in lateral F-SCs, but this asymmetry diminished in more medial F-SCs, as did the elliptical HS shape and RS asymmetry. Variations in DC thickness are also evident in F-SC images from sea otters, bearded seals, northern elephant seals, tammar wallabies, and West Indian Florida manatees but are not explicitly discussed [Marotte et al., 1992; Reep et al., 2001; Marshall et al., 2006; 2014a; McGovern et al., 2015]. DC asymmetries appear correlated to microstructural factors [e.g., RS and SG size; Ling, 1966], as well as muscle attachment. A southern elephant seal study suggested that thinner DC portions in the F-SC functioned to accommodate increased RS and SG sizes [Ling, 1966]. Since harp seal SGs were located in the UCS in a rather even distribution, our results cannot specifically support the SG hypothesis. However, our results support the RS aspect because both the larger RS area and the thinner DC layer were medially located. In addition, we observed

markedly thin DC areas at the extreme basal ends of lateral F-SCs, but the DC thickness was reasonably consistent throughout the LCS in medial F-SCs (Figures 15 and 16). We propose that the basal DC thinning is the result of muscle attachment. Carnivore representatives, domestic cats (*Felis catus*) and dogs (*Canis lupus familiaris*), possess intrinsic and extrinsic muscles to aid in vibrissal movement. Intrinsic muscles are striated and protract vibrissae [Figure 25; Muchlinski et al., 2013]. Striated muscle fibers, likely intrinsic muscles, have been observed attaching to the F-SC base in several pinniped species, including bearded and southern elephant seals, but arrector pillar muscles have only been noted in ringed seals [Ling, 1966; Marshall et al., 2006; Hyvärinen et al., 2009; Marshall et al., in press]. Histological sections from a neonatal tree shrew (*Tupaia glis belangeri*) show a thin DC at the intrinsic muscle attachment site [Figure 26; Muchlinski et al., 2013]. Because shrews, and most rodents, exhibit "whisking" behavior (i.e. rapidly sweeping vibrissae back and forth), they do not have directly comparable mystacial musculature to carnivorans. However, it should be noted that rats rhythmically move their heads while exploring an object, which allows them to physically place their microvibrissae on the object, while their lateral macrovibrissae do the whisking [Hartmann, 2001]. Moreover, this study showed that rats can use their micro- and macrovibrissae consecutively [Hartmann, 2001]. Besides being a great example of the functional differentiation of micro- and macrovibrissae in rodents, this example also alludes to the fact that carnivoran microvibrissae musculature and function could differ from that of their macrovibrissae but have not been investigated systematically.

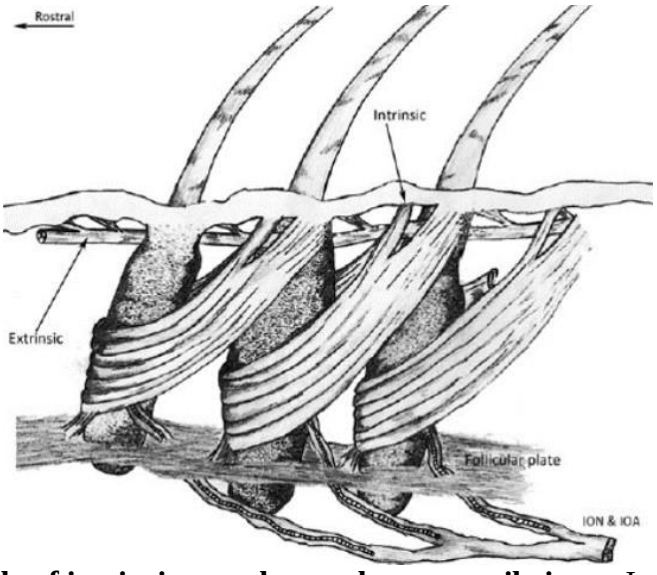


**Figure 25. Example of intrinsic muscle attachment to vibrissae.** Image depicting the medial attachment of intrinsic muscles to F-SCs in a white mouse, *Mus musculus* [ION: Infraorbital nerve, IOA: Infraorbital artery; Muchlinski et al., 2013]*.

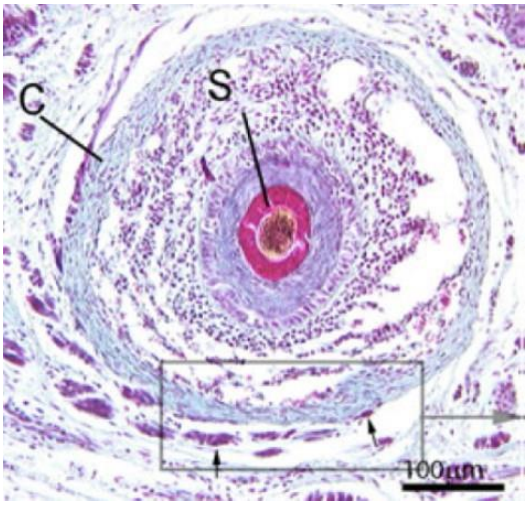


**Figure 26. Cross-section of a neonatal tree shrew F-SC.** Image highlights the location of intrinsic muscle attachment with small black arrows. Note the thinner DC section near muscle attachment location [C: Dermal capsule, S: Hair shaft; Muchlinski et al., 2013]*.

* Both images were reprinted with permission from "Comparative histomorphology of intrinsic vibrissa musculature among primates: implications for the evolution of sensory ecology and 'face touch'" by Muchlinski MN, Durham EL, Smith TD, Burrows AM, 2013. American Journal of Physical Anthropology, 150, 301-312, Copyright 2012 by Wiley Periodicals, Inc.

This potential for a functional difference between micro- and macrovibrissae may help explain the lack of pronounced DC thinning at the basal end of medial F-SCs. However, it is probable that HS morphology and the physics behind HS movement are also key contributors. Medial F-SCs have proportionally shorter HSs given the size of the F-SC than lateral F-SCs (Tables 1-3). Ratios of the mean F-SC lengths to the mean HS lengths of medial (column 2-3) and lateral (column 10) vibrissae were approximately 1:4 and 1:7.5, respectively. Hence, when seals protract their vibrissae while swimming, lateral vibrissae must overcome comparatively more force from the water than medial vibrissae. Subsequently, lateral vibrissae would require more intrinsic musculature, which is reflected in their more distinct, basal DC thinning.

The physical dynamics of HS movement within the F-SC also likely affect F-SC microanatomy. It has been suggested that the HS has three separate fulcrums: 1) the hair papilla, 2) the mouth of the F-SC, and 3) the trabeculae in the upper part of the cavernous sinus in the F-SC. The third fulcrum was originally proposed for terrestrial animals (as they only have one cavernous sinus), but the upper LCS trabeculae would be the equivalent fulcrum location in pinnipeds [Vincent, 1913; Rice et al., 1986; Rice, 1993; Dehnhardt et al., 1999]. The mechanical dynamics within the F-SC are undeniably complex. However, in general, the bending of the HS from forward swimming movement is proposed to compress the leading edge of the F-SC, while simultaneously stretching the remaining caudal portion [Dehnhardt et al., 1999]. In addition, physics dictates that the largest force generated from the HS bending would be localized at the fulcrums. In the case of the first fulcrum, the force of the HS bending is likely countered

by the intrinsic musculature of the vibrissae and relates back to our proposed basal DC thinning hypothesis. In regards to the second fulcrum, Australian water rats have a dense network of trabeculae on the caudal side of their F-SC, which has been posited as a means of compensating for the force of the HS bending [Dehnhardt et al., 1999]. The DC thickening in harp seals on the caudal side of their lateral F-SCs likely serves a similar purpose. Other diving mammals also share this thickened DC trait [e.g., northern elephant seals, sea otters; Marshall et al., 2014a; McGovern et al., 2015], thereby supporting the theory that the added resistance of water during diving contributes to DC thickening [Dehnhardt et al., 1999]. If systematically measured, DC thickness discrepancies in terrestrial or non-diving marine mammals (e.g., West Indian Florida manatees) are predicted to be less variable than those in diving mammals. Any DC thinning in these species would likely be the result of muscle attachment and/or the F-SC accommodating any increases in RS size. In the case of the third fulcrum, the largest force would be at the RS level, where the majority of mechanoreceptors are located.

Similar to the DC, axons bundles were more asymmetrically distributed in lateral F-SCs, but became progressively more symmetrical in medial F-SCs. Axon bundle asymmetry may be dependent on muscle attachment to the F-SC or a myriad of other factors, including flexural stiffness, HS morphology, vibrissal angle of orientation, and/or HS curvature. Based on current data, when vibrissae are protracted underwater, water flow initially contacts the narrow edge of the elliptical HS and flows back across the major axis [Hanke et al., 2010; Murphy et al., 2013; Ginter-Summarell et al., 2015], similar to airflow over an aircraft's wing. In this $0^{o}$ orientation, with the major HS axis

oriented rostral-to-caudal, vibrissae exhibit their highest flexural stiffness and lowest vibration velocity, but opinions vary [Hanke et al., 2010; Murphy et al., 2013; Ginter-Summarell et al., 2015]. Notably, HSs without beads are generally more rigid [Ginter-Summarell et al., 2015]. One study proposed that by negating self-induced vibrations in the $0^o$ orientation, vibrissae are more sensitive to water flow disturbances at a $90^o$ angle [i.e., dorsoventrally and lowest flexural stiffness; Murphy et al., 2013; Ginter-Summarell et al., 2015].

It is hypothesized that the directionally-dependent flexural stiffness properties of HSs could make F-SCs directionally sensitive to water flow as well, subsequently affecting their innervation patterns [Ginter-Summarell et al., 2015]. If axon distribution is considered a proxy for mechanoreceptor distribution, our results support both the flexural stiffness and vibration velocity hypotheses of Ginter-Summarell *et al*. [2015] and Murphy *et al.* [2013] since vibrissae with elliptical HSs had more pronounced axon bundles dorsally. Moreover, it has been shown that almost circular HSs have nearly isotropic, or directionally independent flexural stiffness [Ginter-Summarell et al., 2015], which was highlighted in our medial, nearly circular vibrissae exhibiting less drastic axon bundle asymmetries. However, these hypotheses do not explain why axon bundle distribution was not equally dominant ventrally within F-SCs with elliptical HSs (as it is also at a $90^o$ angle). While asymmetrical axon bundle distribution may indicate directionality within the F-SC, ultimately it is the functional neural unit of the F-SC, the mechanoreceptors, that determines directional stimulation within the F-SC. Different degrees of HS deflection lead to variations in mechanical force within the F-SC and

therefore varying intensities of mechanoreceptor stimulation [Dehnhardt and Dücker, 1996]. Our discussion is based on the assumption that axon bundle distribution is a proxy for mechanoreceptor location and relative directional sensitivity. Although we cannot confirm this assumption within the constraints of this study, we think it is a reasonable assumption, but validation requires future electron microscope analyses.

HS diameter ratio could also affect axon bundle asymmetry. Most mystacial vibrissae studies on elliptically shaped HSs do not specifically comment on the symmetry of axon bundle distribution, making it difficult to draw broader conclusions [Stephens et al., 1973; Marshall et al., 2006; Hyvärinen et al., 2009; McGovern et al., 2015]. However, preliminary data for California sea lions and harbor seals indicate that their F-SCs also possess asymmetrically distributed axon bundles around the HS as the DVN branches to innervate the F-SC [unpublished data]. Vibrissal studies elaborating on axon bundle distribution around circular HSs are equally sparse but most support our theory by showing more evenly distributed bundles around the RS in their figures [i.e., West Indian Florida manatee, sea otter, tammar wallaby; Sprague-Dawley rats (*Rattus norvegicus*); Rice et al., 1986; Marotte et al., 1992; Reep et al., 2001; Marshall et al., 2014a].

The angle of vibrissae orientation while protracted can greatly affect vibrissal vibration velocities and frequencies [Murphy et al., 2013]. Consequently, it is likely that an increased use in specific angles of orientation could help explain our observed asymmetrical axon distribution and support mechanoreceptor directionality. HS curvature could also be a variable since harbor seal vibrissae curve more caudally, while

California sea lion vibrissae are known to curve more ventrally [Murphy et al., 2013]. Although no studies have specifically described the distribution of axon bundles in California sea lion F-SCs, preliminary data indicate that they also have asymmetrical bundles [Sprowls C and Marshall CD, personal communication]. Further analysis would be needed to determine if their axon bundle orientation varies from what was observed in our harp seal F-SCs.

Apocrine sweat glands have been reported in Ross seal F-SCs, as well as in both southern and northern elephant seal F-SCs [Ling, 1966; 1972; McGovern et al., 2015]. Although harp seals possess sparsely distributed apocrine sweat glands superficial to their SGs along their general body surface [Ling, 1965; Khamas et al., 2012], we did not observe any apocrine sweat glands within the F-SC. It is suggested that apocrine sweat glands, which are more developed and extensive in otariids, play a thermoregulatory or chemosensory role [Ling, 1965; Hardy et al., 1991; Khamas et al., 2012; McGovern et al., 2015].

Extensive SGs and secretion ducts were found located apically in the UCS of our harp seal F-SCs. This SG location is similar to that seen in other pinnipeds [Ling, 1966; 1972; Marshall et al., 2006; McGovern et al., 2015]. SGs secrete lipid deposits and are enlarged in the general body surface tissues of phocids. It is thought that more heavily-pelaged pinnipeds mainly use sweat glands for thermoregulation. However, minimally-pelaged phocids are proposed to use SGs for water-proofing their fur, while thermoregulation is instead satisfied with blubber storage [Ling, 1965; Khamas et al., 2012].

The dimples observed on several F-SCs were similar to those reported by Hyvärinen [1989] for ringed seals. It was suggested that these dimples could help vibrissae function individually and aid in water resistance [Hyvärinen, 1989]. Since these dimples were mainly observed on only one harp seal vibrissal pad, we determined them to be artifacts. However, the re-purposed use of the dimples as fiducial marks was beneficial for determining orientations of F-SC microstructures.

## 4.3 *F-SC Innervation*

Emerging comparative innervation studies on mystacial vibrissae support that the terrestrial-to-aquatic transition is related to vibrissal innervation, with increased F-SC innervation observed in more aquatic carnivoran mammals (Table 6). Current innervation estimates show that F-SCs of terrestrial mammals such as rodents, rabbits (*Oryctolagus cuniculus*), cats, monkeys (*Macaca sp.*), and pole cats (*Mustela putorius*) possess 100-200 axons [Rice et al., 1986; Halata and Munger, 1980; Hyvärinen et al., 2009; Lee and Woolsey, 1975]. Semi-aquatic species have 300-600 axons/F-SC (~3x more than terrestrial mammals), while some fully aquatic species possess 1300-1600 axons/F-SC (~10x more than terrestrial mammals) and the highest innervation investment among mammals. However, some fully aquatic mammals (i.e., cetaceans and sirenians) are exceptions to this trend and have diminished mystacial vibrissae innervation compared to pinnipeds. Yet, upon further inspection, these exceptions are complemented by either other well-developed sensory modalities or have evolved divergent tactile sensory systems. Odontocetes evolved echolocation, specializing in

acoustics at the expense of tactile systems, whereas sirenians greatly modified and expanded their vibrissal fields to include the entire body, thus becoming tactile model systems [Marshall et al., 1998a; b; Reep et al., 2002; 2011]. These unique, specialized sensory systems may stem from the fact that cetaceans and sirenians returned to an aquatic habitat in the early to mid-Eocene (~50 mya), approximately 25 million years before the first accepted pinnipedimorph, *Enaliarctos,* did [Berta et al., 2006; Berta, 2009]. Mysticetes (who retain vibrissae) and odontocetes diverged from archaeocetes (earliest whales) ~10 million years before *Enaliarctos* proliferated [Arnason et al., 2004; Berta et al., 2006]. However, echolocation in odontocetes did not evolve until the Oligocene, around the same time *Enaliarctos* emerged [Fleischer, 1976; Berta, 2009]. While odontocete hearing is adapted to detect high-frequency sounds for foraging and other functions of sensing the environment, mysticete hearing organs evolved to perceive low-frequency noises [Fleischer, 1976]. Perhaps because mysticetes did not adapt their hearing abilities for a foraging function, they retained their vibrissae through their adult lives. Sirenians appear to have the most developed vibrissal system among mammals because they have evolved it over the longest period of time and managed to assign their vibrissae an additional foraging function [i.e., oripulation, or using lips and bristles to grasp food; Marshall et al., 1998a; b; Reep et al., 2001]. These data suggest that a phylogenetic signal is present and constrains overall vibrissal patterns. Furthermore, data suggest that foraging strategies play a crucial role in determining if vibrissae were a sensory system selected for in the first place, as well as what vibrissal distribution, microanatomy, and innervation are present in extant mammals today.

Overall, our axon counts from harp seal macrovibrissae were comparable to those reported in other pinniped vibrissal studies. Lateral vibrissae yielded a mean of 1533 ± 192.9 axons/F-SC. Extrapolating by the mean number of F-SCs, we estimate that 147,226 axons innervate the entire harp seal mystacial array. These estimates are similar to estimates from other marine mammals, including sea otters, a close mustelid relative that did not return to a fully aquatic environment until the early Pleistocene [~2 mya; Table 6; Mitchell, 1966; Marshall et al., 2014a]. These data support the hypothesis that the number of axons in large, ventrocaudal vibrissae do not vary substantially among harp seals and other phocids. Furthermore, this estimate corroborates the general 1:3:10 trend of increasing vibrissal innervation observed in terrestrial, semi-aquatic, and fully aquatic mammals, respectively [exempting West Indian Florida manatees and cetaceans; Hyvärinen et al., 2009; Marshall et al., 2014a].

**Table 6**. **Summary of current axon estimates for extant mammals.** Terrestrial (green-shaded cells), semi-aquatic (beige-shaded cells), and fully aquatic (blue-shaded cells) mammals are listed.

| Species | Total Number Mystacial Vibrissae | Mean Number of Axons/F-SC | Total Number of Axons/Array | Citation |
|---|---|---|---|---|
| Pole cats (*Mustela putorius*) | 80 | 110 | 15,000 | Hyvärinen et al., 2009 |
| Domestic Cats (*Felis catus*) | 58 | 175 | 10,159 | Rice et al., 1986; Nomura et al., 1986 |
| European otters (*Lutra lutra*) | 160 | 350 | 72,000 | Hyvärinen et al., 2009 |
| Harp seals (*Pagophilus groenlandicus*) | 90-98 | 1,100 | 100,000 | Yablokov and Klevezal, 1962 |
| Harp Seals (*Pagophilus groenlandicus*) | 96 | 1,533 | 147,226 | Mattson and Marshall (Lateral only) |
| | | 1,221 | 117,235 | Mattson and Marshall (Medial-to-lateral) |
| Northern elephant seals (*Mirounga angustirostris*) | 101 | 1,584 | 159,097 | McGovern et al., 2015 |
| Ringed seals (*Phoca hispida*) | 110 | 1,540 | 169,400 | Hyvärinen and Katajisto, 1984; Hyvärinen, 1995; Hyvärinen et al., 2009 |
| Bearded seals (*Erignathus barbatus*) | 244 | 1,314 | 320,616 | Marshall et al., 2006 |
| Sea otters (*Enhydra lutris*) | 120.5 | 1,339 | 161,313 | Marshall et al., 2014a |
| West Indian Florida manatee (*Trichechus manatus latirostris*) | 152 | 72 (U1), 225 (U2), 102 (U3), 94 (U4) | 20,222 | Reep et al., 2001 |

Innervation differences are arguably the easiest aspect to compare between micro- and macrovibrissae given that they yield comparable numerical values among mammals. Current medial-to-lateral vibrissal axon counts on available species support the need to analyze pinniped macro- and microvibrissal fields separately (Table 7). F-SC axon counts for the terrestrial tammar wallaby range from 116-220 (smaller, medial) to 211-292 [larger, lateral; Marotte et al., 1992]. Sprague-Dawley rats have mean axon counts of 108 (medial) and 152 (lateral) per F-SC [Rice et al., 1986], and Swiss Webster mice (*Mus musculus*) axon counts range between 69 (medial) to 162 (lateral) per F-SC [Lee and Woolsey, 1975]. When F-SCs were compared across the muzzle of Swiss Webster mice, the number of axons innervating F-SCs exhibited a regular, progressive decline [Lee and Woolsey, 1975]. As a semi-aquatic mammal, Australian water rats have axon counts of 363, 450, and 537 per F-SC in their smaller/medial, intermediate, and larger/lateral vibrissae, respectively [Dehnhardt et al., 1999]. These data suggest that fully aquatic mammals would also exhibit innervation differences between their medial and lateral vibrissae, but more information is needed.

Ringed seals and West Indian Florida manatees are the only fully aquatic species with reported medial and lateral vibrissae axon counts. Ringed seals appear to have 1050 axons/F-SC in their medial vibrissae [Hyvärinen et al., 2009], while West Indian Florida manatees possess considerably fewer axons per F-SC (Table 7). It is not clear exactly which medial F-SCs were analyzed for the ringed seal axon count, thereby making it difficult to compare them to our harp seal counts [Hyvärinen et al., 2009]. However, based on our results, we hypothesize that the ringed seal vibrissae were sampled from

column 4. West Indian Florida manatees are rather unique and exhibit vibrissae (and only vibrissae) along the entirety of their body, a feature thought analogous to the lateral line in fish [Reep et al., 2002]. West Indian Florida manatees possess six distinct fields of perioral bristles, with the U1-U4 vibrissal fields being synonymous to other mammalian mystacial vibrissae. U1-U4 vibrissae are organized progressively across the muzzle, with U1 being the most lateral. Unlike pinnipeds whose most lateral vibrissae are the largest, U2 vibrissae are the largest in West Indian Florida manatees and exhibit the highest innervation (210-254 axons/F-SC). The added importance of U2 vibrissae may be related to the fact that West Indian Florida manatees primarily rely on these vibrissae during both tactile exploration (sensory) and foraging (i.e., oripulation, motor). These factors, especially oripulation, could help explain why West Indian Florida manatees developed divergent F-SCs innervation investment and do not have the same medial-to-lateral innervation gradient as that seen in other fully aquatic mammal F-SCs. Medial U4 vibrissae are the smallest and possess 88-100 axons/F-SC [Table 7; Reep et al., 2001]. At the level of the RS, F-SC innervation densities for West Indian Florida manatees showed a significant, positive linear correlation between axon counts and F-SC size across several vibrissal fields [Reep et al., 2001]. Excluding West Indian Florida manatees, the increased innervation trend seen in aquatic mammals is still apparent when focusing on medial and lateral vibrissae (Table 7).

**Table 7. Medial-to-lateral axon count means for several mammals.** Terrestrial (green-shaded cells), semi-aquatic (beige-shaded cells), and fully aquatic (blue-shaded cells) mammals are listed.

| Species | Axon counts/F-SC of smaller, medial vibrissae | Axon counts/F-SC of larger, lateral vibrissae | Citation |
|---|---|---|---|
| Sprague-Dawley rats (*Rattus norvegicus*) | 108 | 152 | Rice et al., 1986 |
| Swiss Webster mice (*Mus musculus*) | 69 | 162 | Lee and Woolsey, 1975 |
| Tammar wallaby (*Macropus eugenii*) | 116-220 | 211-292 | Marotte et al., 1992 |
| Australian water rats (*Hydromys chrysogaster*) | 363 | 537 | Dehnhardt et al., 1999 |
| West Indian Florida manatee (*Trichechus manatus latirostris*) | 94 (U4) | 225 (U2) | Reep et al., 2001 |
| Ringed seal (*Phoca hispida*) | 1,050-1,200 | 1,540 | Hyvärinen et al., 2009 |
| Harp seal (*Pagophilus groenlandicus*) | 550 | 1,632 | Mattson and Marshall |

Including macro- and microvibrissae of harp seals, axon counts from medial-to-lateral F-SCs ranged from 550 ± 97.4 axons/F-SC (column 1) to 1632 ± 173.2 axons/F-SC (column 10), with a mean of 1221 ± 422.3 axons/F-SC and a total innervation to the entire mystacial vibrissal array of 117,235. This value is ~17% greater than previously suggested for harp seals [100,000 axons/mystacial array; Yablokov and Klevezal, 1962]. Moreover, the overall innervation per F-SC mean is still close to 1300 axons/F-SC, which still fits into the 1:3:10 innervation ratio. Including progressive medial-to-lateral

F-SC innervation counts decreased our overall mystacial array estimate for harp seals by 20%. These data support the hypothesis that the total number of axons innervating the entire harp seal mystacial vibrissal field is less than values reported for other phocids when the medial-to-lateral aspect is included. This fact stresses the importance of including medial vibrissae in innervation estimate analyses. The 20% variation is likely applicable across phocids and perhaps all pinnipeds and would result in a downward estimate of already published innervation investment studies. However, innervation estimates in previously published literature have been quantified using stained sections. Although the specific type of stain utilized may vary, it is likely that all staining procedure also produced some degree of tissue stretching, shrinking, and/or expanding. Our stained versus wet comparison indicates that current axon count estimates from stained sections may be ~10% lower than the actual number of axons within the F-SC. Hence, we posit that currently published innervation studies report innervation estimates that are ~10% higher than the more reflective medial-to-lateral, unstained estimates. These percentage discrepancies would not change the overall innervation pattern and conclusions of these studies, but we do strongly suggest that future studies use unstained sections for innervation quantification and that medial F-SCs are included in analyses.

Our harp seal axon counts increased with F-SC surface area, ranging from ~550 (medial) to ~1630 (lateral). Terrestrial species possess medial axon counts between ~70-100 axons/F-SC, whereas a semi-aquatic water rat has ~350 axons/F-SC (Table 7). Hence, medial F-SC axon counts among mammals as they become more aquatic are closer to a 1:3:5 ratio, as opposed to the 1:3:10 ratio found for lateral F-SCs. Differential

innervation between macro-and microvibrissae was high in harp seals (3.0x) compared to West Indian Florida manatees and Swiss Webster mice, (~2.3x), as well as compared to tammar wallabies, Sprague-Dawley rats, Australian water rats, and ringed seals [~1.4x; Lee and Woolsey, 1975; Rice et al., 1986; Marotte et al., 1992; Dehnhardt et al., 1999; Reep et al., 2001]. While they have comparable lateral F-SC axon counts, ringed and harp seals show a prominent difference in medial F-SC counts relative to each other. This discrepancy is not easily explained, especially considering the similar foraging strategies between these species. One explanation could be that it is not clear exactly from which row or column the medial ringed seal vibrissae were dissected [Hyvärinen et al., 2009]. However, the medial axon counts proposed for ringed seals would conserve the 1:3:10 innervation trend observed in lateral F-SCs.

Our observations on medial-to-lateral innervation investment in harp seal F-SCs highlight the importance of all F-SCs to the function of the mystacial array. It is possible that the harp seal mystacial vibrissal array could plausibly be considered to have three distinct vibrissal fields because axon counts appear to plateau from columns 5-8 and columns 9-11 (Figure 20). However, since axon counts exhibit substantial overlap within these columns, we suggest that vibrissal columns 5-11 are considered macrovibrissae and columns 1-4 are categorized as microvibrissae until additional data become available. It is important to mention that this proposed column separation would re-categorize previously defined “medial” vibrissae (e.g. column 7 vibrissae, Figure 3) as lateral, macrovibrissae.

The relationship between F-SC surface area and axon count best fit a generalized non-linear least squares model that began to reach an asymptote at larger, lateral F-SCs (Figure 22). Therefore, these data do not support the hypothesis that the number of axons per F-SC show a positive linear correlation with vibrissal surface area from small, medial vibrissae to large, lateral vibrissae. Instead, a power relationship exists. Our results are similar to data reported for Swiss Webster mice that showed a regular, progressive increase in axon counts in larger F-SCs [Lee and Woolsey, 1975]. We hypothesize that our observed non-linear relationship indicates that mechanoreceptors reach a maximum carrying capacity in larger F-SCs.

Mechanoreceptors could be attaining a carrying capacity due to the combination of HS morphology, HS flexural stiffness, and directionally-sensitive mechanoreceptors. These factors could be forcing mechanoreceptors in larger F-SCs to preferentially over-populate one side, thereby reducing available space for additional mechanoreceptors on that side. In view of the pronounced axon bundle asymmetry in harp seal F-SCs and our assumption that axons are a proxy for mechanoreceptor distribution, we suggest that larger F-SCs reach an innervation asymptote sooner than expected given their overall size because they are more directionally-dependent. Moreover, we posit that innervation increases in vibrissae with asymmetrical axon bundles would be the result of an increase in vertical length, increases in the LCS, RS, and/or ICB. Increasing vertical length would allow for more space for mechanoreceptors on the side of the F-SC that would best maximize sensory perception from the predominant vibrissa deflection angle. In contrast, in F-SCs with symmetrical axon bundles, innervation increases may depend

more on increases in total LCS, RS, and/or ICB surface area and the innervation vs. F-SC size relationship is more likely to be linear. Since the RS and the ICB is where most mechanoreceptors terminate, they are likely the most influential.

Our hypotheses on the limiting factors affecting mechanoreceptor capacity are supported by West Indian Florida manatee data and the fully aquatic mammal data listed in Table 8. West Indian Florida manatee F-SCs have symmetrically distributed axon bundles and exhibit a linear relationship between axon count and both RS perimeter and RS area [Reep et al., 2001]. Sea otter F-SCs also appear to have more symmetrical axon bundles, as well as a surprising number of axons considering the size of their F-SC [Marshall et al., 2014a]. The RS in northern elephant seal F-SCs comprises only ~13% of the total sinus length, but northern elephant seals have the largest F-SC diameter of the pinnipeds compared, giving them the greatest RS surface area estimate. Despite their substantially larger RS surface area, northern elephant seal F-SCs exhibit axon counts in the same range as bearded and harp seals. Although not directly commented on in the literature, northern elephant seal F-SC images indicate that they have somewhat asymmetrical axon bundles. Furthermore, mean max RS lengths in harp, bearded, and northern elephant seal F-SCs were similar at 2.2mm, 2.3mm, and 2.5mm, respectively, supporting the fact that vertical RS space may be a key factor driving mechanoreceptor capacity and equalizing axon counts per F-SC.

Our harp seal data, as well as data from the literature, support that mechanoreceptors may be over-populating one side of marcovibrissae F-SCs because innervation appears to be asymmetrical and constricted by vertical RS space, as more

horizontal RS space still seems to be available (especially evident in northern elephant seals). Since directional dynamics are so integral to vibrissal function, we hypothesize that increasing mechanoreceptors in the less populated RS areas of F-SCs with asymmetrical bundles (if available at all) might not directly translate into increased sensory perception because it would not be biologically useful. Further research that traces individual axon branches and identifies mechanoreceptor type and distribution within the F-SC is needed to verify these hypotheses.

**Table 8. Fully aquatic mammal F-SC proportions and innervations.** RS and LCS percentages for bearded seals and sea otters are the published max RS and LCS means divided by the total F-SC sinus length. Surface area estimates were obtained by calculating the surface area of a cylinder using F-SC diameters and RS lengths listed in the literature. For consistency, only macrovibrissae were compared.

| Species | Mean % UCS | Mean % RS | Mean % LCS | Mean Max F-SC Length (mm) | Axon Count per F-SC | Estimated RS surface area ($mm^2$) | Citation |
|---|---|---|---|---|---|---|---|
| Harp seal | 59.2 ±4.2 | 18.1 ±2.4 | 31.1 ±3.0 | 12.7 ±1.5 | 1,533 | 21.8 | Mattson and Marshall |
| Northern elephant seal | 47.3 ±2.5 | 13.9 ±1.6 | 36.6 ±2.1 | 20.0 ±1.7 | 1,584 | 34.2 | McGovern et al., 2015 |
| Bearded seal | 56.0 ±4.2 | 13.1 | 30.1 | 19.1 ±1.8 | 1,314 | 21.0 | Marshall et al., 2006 |
| Sea otter | 39.4 ±3.2 | 23.1 | 44.9 | 9.9 ±1.2 | 1,339 | 11.9 | Marshall et al., 2014a |

Harp seal F-SC axon densities across the mystacial vibrissal array were inconclusive. These results are contrary to axon densities reported for West Indian

Florida manatees, which showed a positive linear correlation between axon count and F-SC size [Reep et al., 2001]. Variances between harp seal and West Indian Florida manatee axon density data could possibly stem from the previously mentioned mechanoreceptor distribution and/or the complexity of the West Indian Florida manatee vibrissal array. The West Indian Florida manatee data were compiled from all perioral vibrissal fields (i.e., upper and lower jaw bristles, bristle-like hairs near the supradisk region, supradisk, and chin), not just mystacial. No relationship between F-SC size and innervation was discovered in bearded seal F-SCs either [Marshall et al., 2006]. Although we expected harp seal axon densities to mirror those of West Indian Florida manatees, our results are not surprising considering pinniped vibrissae of varying sizes (excluding the most dorsal vibrissal row) have been shown to be similarly represented within the somatosensory cortex [Ladygina et al., 1985]. Since the idea of cortical magnification asserts that more important tactile structures are represented as larger areas in the somatosensory cortex, it makes sense that our F-SCs had similar axon densities [Daniel and Whitteridge, 1961; Catania, 2007].

We located presumptive MNCs at the GM and ORS interface throughout the LCS, RS, and ICB, locations which correspond well to current literature findings, including some for terrestrial species [Stephens et al., 1973; Rice et al., 1986; Marotte et al., 1992; Hyvärinen, 1995; Dehnhardt et al., 1999; Marshall et al., 2006; Sarko et al., 2007; Marshall et al., 2014a; McGovern et al., 2015; Sarko et al., 2015]. MNCs are slowly-adapting mechanoreceptors that are innervated by low-threshold Aβ fibers and are primed to detect changes in pressure and direction [Rice et al., 1986; Lichtenstein et

al., 1990; Halata, 1993; Hyvärinen, 1995; Fleming and Luo, 2013]. For most fully aquatic species (i.e., West Indian Florida manatees, California sea lions, bearded seals, northern elephant seals, sea otters), the RS and ICB were the main location for presumptive MNCs, but some studies also noted them in the LCS [sea otters, northern elephants seals, bearded seals; Stephens et al., 1973; Hyvärinen, 1995; Marshall et al., 2006; Sarko et al., 2007; Marshall et al., 2014a; McGovern et al., 2015]. West Indian Florida manatees and California sea lions F-SCs were observed to have MNCs fully encircling the HS in a uniform fashion at the RS level [Stephens et al., 1973; Sarko et al., 2007]. In West Indian Florida manatees, this dense distribution of MNCs was innervated by heavily branching Aβ fibers [Reep et al., 2001; Sarko et al., 2007]. However, most of the MNCs located within West Indian Florida manatee perioral F-SCs lacked innervation. This intriguing feature was suggested to be due to an increased turnover rate in MNCs [Sarko et al., 2007]. It is unclear if pinnipeds exhibit this same trait, but this aspect could potentially help explain why harp seal F-SC innervation reached an asymptote.

Presumptive lanceolate endings were observed at the junction of the GM and ORS and were primarily localized at the RS level and upper LCS. However, these mechanoreceptors were more sparsely dispersed than presumptive MNCs. Lanceolate endings at this location are common in other aquatic mammals (i.e., California sea lions, bearded seals, northern elephant seals, sea otters, ringed seals) and Australian water rats [Stephens et al., 1973; Hyvärinen, 1995; Dehnhardt et al., 1999; Marshall et al., 2006; 2014a; McGovern et al., 2015]. In West Indian Florida manatees, lanceolate endings

were widely spaced and innervated by minimally branched Aβ fibers [Sarko et al., 2007]. Lanceolate endings are rapidly-adapting mechanoreceptors that are innervated by low-threshold Aβ fibers and exhibit almost no directional preference. In addition, these receptors function to detect variations in velocity or vibrissal acceleration and deceleration [Gottschaldt et al., 1982; Rice et al., 1986; Lichtenstein et al., 1990; Halata, 1993; Fleming and Luo, 2013].

Presumptive lamellated, or Pacinian, corpuscles have been located in the LCS of bearded seal F-SCs [Marshall et al., 2006]. These corpuscles mainly function to detect acceleration and vibration cues [Halata, 1993; Fleming and Luo, 2013]. In ringed seal F-SCs, presumptive Ruffini corpuscles were observed in the RS area and are likely detecting the tension and stretching of surrounding tissues [Halata, 1993; Hyvärinen, 1995; Fleming and Luo, 2013]. Both Pacinian and Ruffini corpuscles would be innervated by Aβ fibers [Fleming and Luo, 2013]. West Indian Florida manatee and bearded seal studies noted free nerve endings in the LCS, but they were also found throughout the RS and ICB in West Indian Florida manatees [Marshall et al., 2006; Sarko et al., 2007]. Free nerve endings have thin C fibers and perceive pain [Halata, 1993]. It should be noted that our harp seal data, as well as observations from northern elephant and bearded seals, were made using light microscopy and mechanoreceptor identities are presumptive. However, they correspond well to the more detailed electron microscopy and immunofluorescent analyses conducted by Hyvärinen [1995] and Sarko *et al.* [2007].

## 4.4 *Fully Aquatic Mammal Vibrissae Evolution*

Regardless of which overall harp seal mystacial array innervation estimate is considered, it is clear that increasingly aquatic mammals (excluding sirenians and cetaceans) have increased vibrissal innervation investment. Innervation investment variation in pinnipeds, as well as mysticetes and odontocetes, appears to be due to differences in foraging strategies [Ling, 1977; Schwerdtfeger et al., 1984; Czech-Damal et al., 2012; Mercado, 2014; Berta et al., 2015; Drake et al., 2015]. For example, bearded seals, which possess the most vibrissae among phocids, and therefore the highest overall innervation to the mystacial array among phocids, are predominantly benthic foragers [Marshall et al., 2006; 2008]. Current data suggest that several mysticetes have ~300-450 axons/F-SC but that vibrissae quantity and distribution vary by foraging strategy [Japha, 1910; Ling, 1977; Mercado, 2014]. Rorquals, lunge feeders, possess ~15 upper jaw, perioral vibrissae [Ling, 1977]. Gray whales (*Eschrichtius robustus*) possess an intermediate number of vibrissae (~80) and are benthic, suction foragers [Berta et al., 2015], while bowhead whales *(Balaena mysticetus*) are skim feeders and have over 300 perioral vibrissae [Drake et al., 2015]. Most odontocetes, except some river dolphins, lose their vibrissae after birth and instead rely heavily on echolocation [Norris et al., 1961; Ling, 1977; Schwerdtfeger et al., 1984; Thewissen et al., 2011]. Even though many odontocetes depend on echolocation for foraging, Guiana dolphins (*Sotalia guianensis*) retain vibrissal crypts on their rostrums that are innervated by the trigeminal nerve (~300 axons/crypt) and which have transformed to take on an electroreceptive

function [Czech-Damal et al., 2012]. They are the only eutherians mammal to possess this sense.

Because of the number of exceptions to the increased innervation trend for aquatic mammals (e.g., cetaceans and sirenians), it is unlikely that one all-encompassing theme can fully explain the evolution of mammalian vibrissal function. This is not surprising since, as a group, "marine mammals" and especially "aquatic mammals" have different foraging strategies, are not monophyletic, and transitioned back to aquatic habitats at different times. Clearly, each group has a unique evolutionary history. Therefore, it seems probable that vibrissal innervation patterns observed in extant mammals have overarching similarities based on phylogenetic lineage (e.g., Rodentia, Carnivora, Cetacea, Afrotheria) and that these patterns are refined by habitat and foraging ecology. For instance, "whisking" is commonly seen in Rodentia [Mitchinson et al., 2011]. Similar to sirenians, rock hyraxes (*Procavia capensis*), an Afrotherian and close West Indian Florida manatee relative, also have vibrissae distributed over their entire body, not just on the face [Sarko et al., 2015]. Within a specific lineage, F-SC innervation increases based on the degree of a species' aquatic lifestyle (i.e., terrestrial, semi-aquatic, fully aquatic). One pertinent example is the semi-aquatic Australian water rat, which exhibits increased innervation investment over its terrestrial counterparts (Table 7). Interestingly, Australian water rats maintain Rodentia whisking behavior, albeit weak, supposedly due to the increased density of water [Dehnhardt et al., 1999]. Available comparative data suggest that closely related lineages will exhibit a 1:3:10 vibrissal innervation ratio as species become more aquatic [Hyvärinen et al., 2009;

Marshall et al., 2014a], but we hypothesize that this specific ratio will not hold for all lineages. It seems unlikely that rock hyraxes will have 10x less innervation per mystacial F-SC than the 210-254 axons/F-SC seen in their West Indian Florida manatee relatives since even Swiss Webster mice have 69 axons/F-SC in their small, medial vibrissae [Lee and Woolsey, 1975; Reep et al., 2001]. We suspect that, within lineages and habitats, vibrissal innervation patterns vary due to differences in foraging strategies [e.g., lunge, suction, pelagic, benthic feeding; Marshall et al., 2006; Hanke et al., 2013; Berta et al., 2015; Drake et al., 2015]. Our harp seal data fit well within this organizational pattern and contribute to understanding the evolution of hair at the level of foraging strategies among pinnipeds. However, it is evident that additional comparative data placed within a phylogenetic context is needed. This information would allow us to fully grasp how the selective pressures of a terrestrial-to-aquatic transition resulted in the diversity of vibrissal innervation, form, and function observed among extant mammals today.

# 5. CONCLUSIONS

## 5.1 *Summary*

Pinnipeds are renowned for their large and well-developed vibrissal sensory system. Although behavioral experiments on pinnipeds have attempted to pinpoint functional variations in mystacial vibrissae across the muzzle, no microanatomical or innervational studies have systematically analyzed the functional structure of pinniped mystacial vibrissae as a whole. As a result, comparative data are lacking. Consequently, it is challenging to relate pinniped mystacial vibrissae innervation and microanatomy to other mammals, draw inferences about how pinnipeds utilize their vibrissae for prey acquisition, and fully understand the evolution of vibrissae. To contribute to the growing comparative dataset on pinniped vibrissal structure, function, and innervation, we systematically investigated the innervation and microanatomy of harp seal vibrissae, with a focus on variations across the muzzle. Our main hypotheses were: 1) Axon counts in large, ventrocaudal vibrissae do not vary substantially between harp seals and other pinnipeds, 2) the total number of axons innervating the entire harp seal mystacial vibrissal array is less than values reported for other pinnipeds when the medial-to-lateral aspect is included, and 3) the number of axons per vibrissa show a positive linear correlation with vibrissal surface area from small, medial vibrissae to large, lateral vibrissae.

Currently, data suggest that functional differences exist among pinniped mystacial vibrissae, with phocid vibrissae primed to detect hydrodynamic wake trails, while otariids and odobenids are more sensitive to close-up sensations [haptics; Ling,

1972; Kastelein and van Gaalen, 1988; Dehnhardt, 1994; Dehnhardt and Dücker, 1996; Dehnhardt et al., 2001; Berta et al., 2006; Marshall et al., 2006; Ginter et al., 2012; Hanke et al., 2013]. Behavioral experiments also indicate that, within each of these families, a functional difference occurs within the mystacial vibrissae array because pinnipeds reorient their medial, smaller vibrissae onto objects after initially contacting objects with their lateral, larger vibrissae [Kastelein and van Gaalen, 1988; Dehnhardt and Dücker, 1996; Grant et al., 2013]. In essence, behavioral studies indicate that pinniped microvibrissae are best designed for object recognition and haptics, while macrovibrissae are better adapted for distant, vibrational stimuli. Our results support that a distinct vibrissae dichotomy exists not only functionally, but also morphologically. Consequently, it is vital that pinniped vibrissal analyses include considerations for medial microvibrissae (columns 1-4), as well as lateral macrovibrissae (columns 5-11).

Harp seals macro- and microvibrissae possessed: 1) similar general microanatomical structures (e.g., CT, ORS, ICB, location of DVN innervation, mechanoreceptors), 2) a tripartite blood sinus system, 3) similar percentages of the LCS, RS, and UCS, 4) HS beading, and 5) similar RS widths. Compared to macrovibrissae, microvibrissae exhibited: 1) shorter HS and F-SC lengths, 2) more circular HSs, 3) a circular HS shape throughout the LCS, 4) more symmetrical DC thicknesses, 5) more symmetrical axon bundle distribution, 6) more symmetrical RS lengths, and 7) lower axons counts, but similar axon densities. From F-SC orientation analyses we determined that higher densities of axons were distributed dorsally and that both thinner DC portions and larger RS sections were medially located. These results provide the innervational

and microanatomical foundations for understanding the different behavioral manifestations seen in pinnipeds during tactile experiments. In general, our data supported that harp seals have similar vibrissal sensory systems as generalist foragers. However, since no other microanatomical data exist for pinniped microvibrissae, more specific comparisons about the relationship between microvibrissae microstructure and foraging behavior cannot be made at this time.

Microvibrissae and macrovibrissae axon counts ranged from 550 ± 97.4 axons/F-SC (column 1) to 1632 ± 173.2 axons/F-SC (column 10), respectively. Consequently, harp seals have an overall mystacial array innervation of ~117,235 axons. Overall, our data supported our hypotheses that lateral harp seal F-SCs had similar axon counts as those of other pinnipeds and that our innervation estimate to the entire harp seal mystacial vibrissal array was lower than that of other pinnipeds when we included medial axon counts. However, our third hypothesis was not supported. Harp seal F-SCs yielded a non-linear relationship between axon counts and vibrissa surface area.

Our macrovibrissae axon counts fit into a 1:3:10 innervation ratio compared to terrestrial, semi-aquatic, and other fully aquatic mammals, whereas our medial innervations were closer to a 1:3:5 ratio. These innervation data, combined with other morphological and functional differences (e.g., terrestrial mammals and water rats lack an UCS, pinnipeds do not exhibit whisking behavior), suggest that vibrissae evolved differently depending on environmental pressures. The fact that vibrissae likely evolved to serve a strictly sensory function, and that this primary function appears to have been conserved over time, helps account for why species with strong alternative sensory

capabilities have diminished vibrissal sensitivities (e.g., odontocetes and echolocation) and why vibrissae are specifically adapted to a species' foraging requirements (e.g., benthic, suction).

## 5.2 *Recommendations for Future Research*

This thesis confirmed the importance of evaluating mystacial vibrissae separately in pinnipeds, while simultaneously illuminating several avenues for future exploration in vibrissal behavioral experiments, microanatomy, and innervation. Since our data strongly support that a difference exists between medial and lateral vibrissae in pinnipeds, behavioral experiments that isolate either micro- or macrovibrissae at one time would prove beneficial. For instance, conducting an experiment similar to Murphy *et al.*'s [2015] study with a vibrating sheet, but analyzing micro- and macrovibrissae sensitivities separately, could provide useful information that aids in clarifying the discrepancies among the vibrational experiments with similar setups. These types of experiments would allow researchers to understand how micro- and macrovibrissae function individually and apply this knowledge to the sensory perception of the mystacial vibrissal array as a whole. Another helpful future behavioral study would be to analyze the orientation of pinniped vibrissae *in vivo* and how this orientation changes as vibrissae are protracted, retracted, or exposed to certain water trails.

Valuable microanatomical data could be gained from studies that determine if asymmetries and orientations of certain structures (e.g., axon bundles, DC thickness) within the F-SC are conserved throughout the entire mystacial vibrissal array. Further studies examining the microstructure of microvibrissae are warranted. In addition, more

detailed analyses on variations in orientation microstructure within a F-SC (e.g., thinnest DC locations) would be advantageous and offer more information about how F-SCs are adapted to handle the complex force dynamics (e.g., possessing multiple fulcrums, the HS having variable flexural stiffness and morphology at different locations) acting within them.

Further innervation studies would also yield complementary comparative data. Obtaining F-SC axon counts for vibrissae as they progress ventral-to-dorsal across the muzzle would offer even better total innervation estimates. Furthermore, these data would also expand on our speculations about the work of Ladygina *et al.* [1985], who observed that the most extreme dorsal row of vibrissae had a substantially smaller representation in the somatosensory cortex than all other vibrissal rows. While our harp seal data fit the trend of the increasing innervation trend for increasingly aquatic mammals, reports on axon densities in terrestrial and semi-aquatic mammals is of paramount importance for making more direct comparisons among mammals. It may be that, after normalizing for the surface area of the F-SCs, no pronounced differences exist between their innervation investments, thereby making the increased innervation seen in pinnipeds strictly size dependent. Finally, we suggest that more in-depth mechanoreceptor investigations are conducted on both micro- and macrovibrissae, since it is likely that variances in mechanoreceptor type and location exist within the F-SC and could result in potentially significant sensory repercussions.

## LITERATURE CITED


Adam P, Berta A (2002): Evolution of prey capture strategies and diet in the pinnipedimorpha (Mammalia, Carnivora). Oryctos 4:83-107.

Ahlberg PE, Clark JA (2006): A firm step from water to land. Nature 440:747-749.

Andres KH (1966): Über die Feinstruktur der Rezeptoren an Sinushaaren. Z Zellforsch 75:339-365.

Arnason U, Gullberg A, Janke A (2004): Mitogenomic analyses provide new insights into cetacean origin and evolution. Gene 333:27-34.

Arnason U, Gullberg A, Janke A, Kullberg M, Lehman N, Petrov EA, Väinölä R (2006): Pinniped phylogeny and a new hypothesis for their origin and dispersal. Mol Phylogenet Evol 41:345-354.

Beck GG, Hammill MO, Smith TG (1993): Seasonal variation in the diet of harp seals (*Phoca groenlandica*) from the Gulf of St. Lawrence and Western Hudson Strait. Can J Fish Aquat Sci 50:1363-1371.

Berta A, Ray CE, Wyss AR (1989): Skeleton of the oldest known pinniped, *Enaliarctos mealsi*. Science 244:60-62.

Berta A (1991): New *Enaliarctos* (Pinnipedimorpha) from the Oligocene and Miocene of Oregon and the role of "Enaliaretids" in Pinniped Phylogeny. Smith Contrib Paleobiol 69:1-33.

Berta A, Wyss AR (1994): Pinniped Phylogeny. Proc San Diego Soc Nat Hist 29:33-56.

Berta A, Sumich JL, Kovacs K (2006): Marine Mammals: Evolutionary Biology 2nd ed. San Diego, Elsevier Inc.

Berta A (2009): Pinniped evolution; in Perrin WF, Würsig B, Thewissen JGM (eds): Encyclopedia of Marine Mammals 2nd ed. San Diego, Academic Press, pp 861-868.

Berta A, Churchill M (2012): Pinniped taxonomy: review of currently recognized species and subspecies, and evidence used for their description. Mamm Rev 42:207-234.

Berta A, Ekdale EG, Zellmer NT, Deméré TA, Kienle SS, Smallcomb M (2015): Eye, nose, hair, and throat: external anatomy of the head of a neonate gray whale (Cetacea, Mysticeti, Eschrichtiidae). Anat Rec 298:648-659.

Bleckmann H, Breithaupt T, Blickhan R, Tautz J (1991): The time course and frequency content of hydrodynamic events cause by moving fish, frogs, and crustaceans. J Comp Physiol A 168:749-757.

Bodian D (1936): A new method for staining nerve fibers and nerve endings in mounted paraffin sections. Anat Rec 65:89-97.

Bowen WD, Tully D, Boness DJ, Bulheier BM, Marshall GJ (2002): Prey-dependent foraging tactics and prey profitability in a marine mammal. Mar Ecol Prog Ser 244:235-245.

Brecht M, Preilowski B, Merzenich MM (1997): Functional architecture of the mystacial vibrissae. Behav Brain Res 84:81-97.

Butler AB, Hodos W (1996): Comparative Vertebrate Neuroanatomy: Evolution and Adaptation. New York, Wiley-Liss, Inc.

Catania KC (2007): The evolution of the somatosensory system, clues from specialized species; in Kaas JH, Krubitzer LA (eds): Evolution of Nervous System. Amsterdam, Elsevier, vol 3, pp 189-206.

Catania KC (2012): Tactile sensing in specialized predators – from behavior to the brain. Curr Opin Neurobiol 22:251-258.

Chernova OF (2006): Evolutionary aspects of hair polymorphism. Biol Bull 33:43-52.

Czech-Damal NU, Liebschner A, Miersch L, Klauer G, Hanke FD, Marshall C, Dehnhardt G, Hanke W (2012): Electroreception in the Guiana dolphin (*Sotalis guianensis*). Proc R Soc B 279:663-668.

Daniel PM, Whitteridge D (1961): The representation of the visual field on the cerebral cortex in monkeys. J Physiol 159:203-221.

Davidson P, Hardy MH (1952): The development of mouse vibrissae *in vivo* and *in vitro*. J Anat 86:342-356.

Davis RW, Hagey W, Horning M (2004): Monitoring the behavior and multi-dimensional movements of Weddell seals using an animal-borne video and data recorder. Mem Nat Inst Pol Res Spec Issue 58:148-154.

Dehnhardt G (1994): Tactile size discrimination by a California sea lion (*Zalophus californianus*) using its mystacial vibrissae. J Comp Physiol A 175:791-800.

Dehnhardt G, Dücker G (1996): Tactual discrimination of size and shape by a California sea lion (*Zalophus californianus*). Anim Learn Behav 24:366-374.

Dehnhardt G, Mauck B, Bleckmann H (1998): Seal whiskers detect water movements. Nature 394: 235-236.

Dehnhardt G, Hyvärinen H, Palviainen A, Klauer G (1999): Structure and innervation of the vibrissal follicle-sinus complex in the Australian water rat, *Hydromys chrysogaster*. J Comp Neurol 411:550-562.

Dehnhardt G, Mauck B, Hanke W, Bleckmann H (2001): Hydrodynamic trail-following in harbor seals (*Phoca vitulina*). Science 293:102-104.

Dehnhardt G, Mauck B (2008): The physics and physiology of mechanoreception; in Thewissen JGM, Nummela S (eds): Sensory Evolution on the Threshold: Adaptations in Secondarily Aquatic Vertebrates. Berkeley, University of California Press, pp 287-293.

Deméré TA, Berta A (2002): The pinniped Miocene *Desmatophoca oregonensis* Condon, 1906 (Mammalia: Carnivora) from the Astoria formation, Oregon. Smith Contrib Paleobiol 93:113-147.

Dhouailly D (2009): A new scenario for the evolutionary origin of hair, feather, and avian scales. J Anat 214:587-606.

Downs T (1956): A new pinniped from the Miocene of Southern California: with remarks on the Otariidae. J Paleontol 30:115-131.

Drake SE, Crish SD, George JC, Stimmelmayr R, Thewissen JGM (2015): Sensory hairs in the bowhead whale, *Balaena mysticetus* (Cetacea, Mammalia). Anat Rec 298:1327-1335.

Dykes RW (1974): Afferent fibers from mystacial vibrissae of cats and seals. J Neurophysiol 39:650-662.

Eckhart L, Dalla Valle L, Jaeger K, Ballaun C, Szabo S, Nardi A, Buchberger M, Hermann M, Alibardi L, Tschachler E (2008): Identification of reptilian genes encoding hair keratin-like proteins suggests a new scenario for the evolutionary origin of hair. Proc Natl Acad Sci USA 105:18419-18423.

Ebara S, Kumamoto K, Matsuura, Mazurkiewicz J, Rice F (2002): Similarities and differences in the innervation of mystacial vibrissal follicle-sinus complexes in the rat and cat: a confocal microscopic study. J Comp Neurol 449:103-119.

Erdsack N, Dehnhardt G, Hanke W (2014): Thermoregulation of the vibrissal system in harbor seals (*Phoca vitulina*) and Cape fur seals (*Arctocephalus pusillus pusillus*). J Exp Mar Biol Ecol 452:111-118.

Fay F (1982): Ecology and biology of the Pacific walrus, *Odobenus rosmarus divergens* Illiger. N Am Fauna 74:1-279.

Fleischer G (1976): Hearing in extinct cetaceans as determined by cochlear structure. J Paleontol 50:133-152.

Fleming MS, Luo W (2013): The anatomy, function, and development of mammalian Aβ low threshold mechanoreceptors. Front Biol 8:doi:10.1007/s11515-013-1271-1.

George I, Holliday C (2013): Trigeminal nerve morphology in *Alligator mississippiensis* and its significance for crocodyliform facial sensation and evolution. Anat Rec 296:670-680.

Ginter CC, Fish FE, Marshall CD (2010): Morphological analysis of the bumpy profile of phocid vibrissae. Mar Mamm Sci 26:733-743.

Ginter CC, DeWitt T, Fish FE, Marshall CD (2012): Fused traditional and geometric morphometrics demonstrate pinniped whisker diversity. PloS One 7:e34481.

Ginter-Summarell CC, Ingole S, Fish FE, Marshall CD (2015): Comparative analysis of the flexural stiffness of pinniped vibrissae. PloS One 10:e0127941.

Gläser N, Wieskotten S, Otter C, Dehnhardt G, Hanke W (2011): Hydrodynamic trail following in a California sea lion (*Zalophus californianus*). J Comp Physiol A 197:141-151.

Gottschaldt KM, Fruhstorfer H, Schmidt W, Kräft I (1982): Thermosensitivity and its possible fine-structure basis in mechanoreceptors in the beak skin of geese. J Comp Neurol 205:219-245.

Grant R, Wieskotten S, Wengst N, Prescott T, Dehnhradt G (2013): Vibrissal touch sensing in the harbor seal (*Phoca vitulina*): how do seals judge size? J Comp Physiol A 199:521-533.

Greaves D, Hammill M, Eddington J, Schreer J (2004): Growth rate and shedding of vibrissae in the gray seal, *Halichoerus grypus*: A cautionary note for stable isotope diet analysis. Mar Mamm Sci 20:296-304.

Halata Z, Munger B (1980): Sensory nerve endings in rhesus monkey sinus hairs. J Comp Neurol 192:645-663.

Halata Z (1993): Sensory innervation of the hair skin (light- and electronmicroscopic study. J Invest Dermatol 101:75S-81S.

Hallgren KA (2012): Computing inter-rater reliability for observational data: an overview and tutorial. Tutor Quant Methods Psychol 8:23-34.

Hanke W, Witte M, Miersch L, Brede M, Oeffner J, Michael M, Hanke F, Leder A, Dehnhardt G (2010): Harbor seal vibrissa morphology suppresses vortex-induced vibrations. J Exp Biol 213:2665-2672.

Hanke W, Wieskotten S, Marshall C, Dehnhardt G (2013): Hydrodynamic perception in true seals (Phocidae) and eared seals (Otariidae). J Comp Physiol A 199:421-440.

Hardy MH (1951): The development of pelage hairs and vibrissae from skin in tissue culture. Ann NY Acad Sci 53:546-561.

Hardy MH, Roff E, Smith TG, Ryg M (1991): Facial skin glands of ringed and grey seals, and their possible function as odoriferous organs. Can J Zool 69:189-200.

Hartmann MJ (2001): Active sensing capabilities of the rat whisker system. Auton Rob 11:249-254.

Heaslip S, Bowen D, Iverson S (2014): Testing predictions of optimal diving theory using animal borne video from harbour seals (*Phoca vitulina concolor*). Can J Zool 92:309-318.

Hirons AC, Schell DM, St. Aubin DJ (2001): Growth rates of vibrissae of harbor seals (*Phoca vitulina*) and Steller sea lions (*Eumetopias jubatus*). Can J Zool 79:1053-1061.

Hocking DP, Evans AR, Fitzgerald EMG (2013): Leopard seals (*Hydrurga leptonyx*) use suction and filter feeding when hunting small prey underwater. Pol Biol 36:211-222.

Hocking DP, Salverson M, Fitzgerald EMG, Evans AR (2014): Australian fur seals (*Arctocephalus pusillus doriferus*) use raptorial biting and suction feeding when targeting prey in different foraging scenarios. PloS One 9:e112521.

Hu KS, Kwak HH, Song WC, Kang HJ, Kim HC, Fontaine C, Kim HJ (2006): Branching patterns of the infraorbital nerve and topography within the infraorbital space. J Craniofac Surg 17:1111-1115.

Huber E (1930a): Evolution of facial musculature and cutaneous field of trigeminus. Part I. Q Rev Biol 5:133-188.

Huber E (1930b): Evolution of facial musculature and cutaneous field of trigeminus. Part II. Q Rev Biol 5:389-437.

Hyvärinen H, Katajisto H (1984): Functional structure of the vibrissae of the ringed seal (*Phoca hispida* Schr.). Acta Zool Fenn 171:27-30.

Hyvärinen H (1989): Diving in darkness, whiskers as sense organs of the ringed seal (*Phoca hispida saimensis*). J Zool 218:663-678.

Hyvärinen H (1995): Structure and function of the vibrissae of the ringed seal (*Phoca hispida* L.); in Kastelein RA, Thomas JA, Nachtigall PE (eds): Sensory Systems of Aquatic Animals. Woerden, De Spil Publishers, pp 429-445.

Hyvärinen H, Palviainan A, Strandberg U, Holopainen IJ (2009): Aquatic environment and differentiation of vibrissae: comparison of sinus hair systems of ringed seal, otter, and pole cat. Brain Behav Evol 74:268-279.

Ito M, Yang Z, Andl T, Cui C, Kim N, Millar SE, Cotsarelis G (2007): Wnt-dependent *de novo* hair follicle regeneration in adult mouse skin after wounding. Nature 447:316-320.

Japha, A (1910): Die Haare der Waltiere. Zoologische Jahrbücher. Abteil Anat Ontogen Tiere 32:1-42.

Karlsson JOM, Toner M (1996): Long-term storage of tissues by cryopreservation: critical issue. Biomaterials 17: 243-256.

Kastelein RA, van Gaalen M (1988): The sensitivity of the vibrissae of a Pacific walrus (*Odobenus rosmarus divergens*) Part 1. Aquat Mamm 14.3:123-133.

Kelley NP, Pyenson ND (2015): Evolutionary innovation and ecology in marine tetrapods from the Triassic to the Anthropocene. Science 348: doi:10.1126/science.aaa3716.

Kernaléguen L, Cazelles B, Arnould JPY, Richard P, Guinet C, Cherel Y (2012): Long term species, sexual and individual variations in foraging strategies of fur seals revealed by stable isotopes in whiskers. PloS One 7:3e32916

Khamas WA, Smodlaka H, Leach-Robinson J, Palmer L (2012): Skin histology and its role in heat dissipation in three pinniped species. Acta Vet Scand 54: doi:10.1186/1751-0147-54-46.

King J (1983): Seals of the World. Ithaca, Cornell University Press.

Kohno N, Barnes LG, Hirota K (1994): Miocene fossil pinnipeds of the genera Prototaria and Neotherium (Carnivora; Otariidae; Imagotariinae) in the North Pacific ocean: evolution, relationships, and distribution. Island Arc 3:285-308.

Koretsky I, Sanders AE (2002): Paleontology from the late Oligocene Ashley and Chandler bridge formations of South Carolina, 1: Paleogene pinniped remains; the oldest known seal (Carnivora: Phocidae). Smith Contrib Paleobiol 93:179-183.

Labansen A, Lydersen C, Levermann N, Haug T, Kovacs K (2011): Diet of ringed seals (*Pusa hispida*) from Northeast Greenland. Pol Biol 34:227-234.

Ladygina TF, Popov VV, Supin AY (1985): Topical organization of somatic projections in the fur seal cerebral cortex. Neurophysiology 17:246-252.

Lee KJ, Woolsey TA (1975): A proportional relationship between peripheral innervation density and cortical neuron number in the somatosensory system of the mouse. Brain Res 99:349-353.

Lichtenstein SH, Carvell GE, Simons DJ (1990): Responses of rat trigeminal ganglion neurons to movements of vibrissae in different directions. Somatosens Mot Res 7:47-65.

Lindstrøm U, Harbitz A, Haug T, Nilssen K (1998): Do harp seals *Phoca groenlandica* exhibit particular prey preferences? ICES J Mar Sci 5:941-953.

Ling J (1965): Functional significance of sweat glands and sebaceous glands in seals. Nature 208: 560-562.

Ling J (1966): The skin and hair of the southern elephant seal, *Mirounga leonine* (Linn.) Aust J Zool 14:855-866.

Ling J (1972): Vibrissa follicles of the Ross seal. Brit Antarc Surv Bull 27:19-24.

Ling J (1977): Vibrissae of marine mammals; in Harrison RJ (ed): Functional Anatomy of Marine Mammals. London, Academic Press, pp 387-415.

Lundström K, Hjerne O, Lunnerud S, Karlsson O (2010): Understanding the diet composition of marine mammals: grey seals (*Halichoerus grypus*) in the Baltic Sea. ICES J Mar Sci 67:1230-1239.

Lydersen C, Angantyr LA, Wiig O, Øritsland T (1991): Feeding habits of Northeast Atlantic harp seals (*Phoca groenlandica*) along the summer ice edge of the Barents Sea. Can J Fish Aquat Sci 48:2180-2183.

Maderson PFA (1972): When? Why? And How?: Some speculations on the evolution of the vertebrate integument. Am Zool 12:159-171.

Maderson PFA (2003): Mammalian skin evolution: a reevaluation. Exp Dermatol 12:233-236.

Marotte L, Rice F, Waite P (1992): The morphology and innervation of facial vibrissae in the tammar wallaby, *Macropus eugenii*. J Anat 180:401-417.

Marshall CD, Huth GD, Edmonds VM, Halin DL, Reep RL (1998a): Prehensile use of perioral bristles during feeding and associated behaviors of the Florida manatee (*Trichechus manatus latirostris*). Mar Mamm Sci 14:274-289.

Marshall CD, Clark LA, Reep RL (1998b): The muscular hydrostat of the Florida manatee (*Trichechus manatus latirostris)*: a functional morphological model of perioral bristle use. Mar Mamm Sci 14:290-303.

Marshall CD, Amin H, Kovacs K, Lydersen C (2006): Microstructure and innervation of the mystacial vibrissal follicle-sinus complex in bearded seals, *Erignathus barbatus* (Pinnipedia: Phocidae). Anat Rec A 288A:13-25.

Marshall CD, Kovacs KM, Lydersen C (2008): Feeding kinematics, suction and hydraulic jetting capabilities in bearded seals (*Erignathus barbatus*). J Exp Biol 211:699-708.

Marshall CD, Rozas K, Kot B, Gill VA (2014a): Innervation patterns of sea otters (*Enhydra lutris*) mystacial follicle-sinus complexes. Front Neuroanat 8:121 doi:10.3389/fnana.2014.00121.

Marshall CD, Wieskotten S, Hanke W, Hanke FD, Marsh A, Kot B, Dehnhardt G (2014b): Feeding kinematics, suction, and hydraulic jetting performance of Harbor seals (*Phoca vitulina*). PloS One 9(1): e86710.

Marshall CD, Rosen D, Trites AW (in press): Feeding kinematics and performance of basal otariid pinnipeds, Steller sea lions (*Eumetopias jubatus*), and northern fur seals (*Callorhinus ursinus*): implications for the evolution of mammalian feeding. J Exp Biol.

Marshall CD, Goldbogen JA (in press): Marine mammal feeding mechanisms; in Castellini MA, Mellish JA (eds): Marine Mammal Physiology: Requisites for Ocean Living. Boca Raton, CRC Press.

Masson P (1929): Some histological methods. Trichrome stainings and their preliminary technique. J Tech Methods 12:75-90.

Mauck B, Eysel U, Dehnhardt G (2000): Selective heating of vibrissal follicles in seals (*Phoca vitulina*) and dolphins (*Sotalia fluviatilis guianensis*). J Exp Biol 203:2125-2131.

McGovern KA, Marshall CD, Davis RW (2015): Are vibrissae viable sensory structures for prey capture in northern elephant seals, *Mirounga angustirostris*? Anat Rec 298:750-760.

Meng J, Wyss AR (1997): Multituberculate and other mammal hair recovered from Palaeogene excreta. Nature 385:712-714.

Mercado III E (2014): Tubercles: What sense is there? Aquat Mamm 40:95-103.

Miersch L, Hanke W, Wieskotten S, Hanke FD, Oeffner J, Leder A, Brede M, Witte M, Dehnhardt G (2011): Flow sensing by pinniped whiskers. Philos Trans R Soc Lond B Biol Sci 366:3077-3084.

Mills FHJ, Renouf D (1986): Determination of the vibration sensitivity of harbour seal *Phoca vitulina* (L.) vibrissae. J Exp Mar Biol Ecol 100:3-9.

Mitchell ED (1966): Northeastern Pacific Pleistocene otters. J Fish Res Board Can 23:1897-1911.

Mitchell ED, Tedford RH (1973): The Enaliarctinae: a new group of extinct aquatic carnivore and a consideration of the origin of the Otariidae. Bull Am Mus Nat Hist 151:201-284.

Mitchinson B, Grant RA, Arkley K, Rankov V, Perkon I, Prescott TJ (2011): Active sensing in rodents and marsupials. Philos Trans R Soc Lond B Biol Sci doi:10.1098/rstb.2011.0156.

Muchlinski MN, Durham EL, Smith TD, Burrows AM (2013): Comparative histomorphology of intrinsic vibrissa musculature among primates: implications for the evolution of sensory ecology and "face touch." Am J Phys Anthropol 150:301-312.

Murphy CT, Eberhardt WC, Calhoun BH, Mann KA, Mann DA (2013): Effect of angle on flow-induced vibrations of pinniped vibrissae. PloS One 8:e69872.

Murphy CT, Reichmuth C, Mann D (2015): Vibrissal sensitivities in a harbor seal (*Phoca vitulina*). J Exp Biol 218:2463-2471.

Necker R (2000): The somatosensory system; in Whittlow CG (ed): Sturkie's Avian Physiology. New York, Academic Press, pp 57-69.

Nilssen KT (1995): Seasonal distribution, condition and feeding habits of Barents Sea harp seals (*Phoca groenlandica*). Dev Mar Biol 4:241-254.

Nilssen KT, Pedersen OP, Folkow LP, Haug T (2000): Food consumption estimates of Barent Sea harp seals. NAMMCO Sci Pub 2:9-27.

Nomura S, Itoh K, Sugimoto T, Yasui Y, Kamiya H, Mizuno N (1986): Mystacial vibrissae representation within the trigeminal sensory nuclei of the cat. J Comp Neurol 253:121-133.

Norris KS, Prescott JH, Asa-Dorian PV, Perkins P (1961): An experimental demonstration of echo-location behavior in the porpoise, *Tursiops truncatus* (Montagu). Biol Bull 120:163-176.

Parrish F, Craig M, Ragen T, Marshall G, Buhleier B (2000): Identifying diurnal foraging habit of endangered Hawaiian monk seals using a seal-mounted video camera. Mar Mamm Sci 16:392-412.

Pauly D, Trites A, Capuli E, Christensen V (1998): Diet composition and trophic levels of marine mammals. ICES J Mar Sci 55:467-481.

Radinsky LB (1968): Evolution of somatic sensory specialization in otter brains. J Comp Neurol 134:495-506.

Reep RL, Stoll ML, Marshall CD, Homer BL, Samuelson DA (2001): Microanatomy of facial vibrissae in the Florida manatee: The basis for specialized sensory function and oripulation. Brain Behav Evol 58:1-14.

Reep RL, Marshall CD, Stoll ML (2002): Tactile hairs on the postcranial body in Florida manatees: A mammalian lateral line? Brain Behav Evol 59:141-154.

Reep RL, Gaspard III JC, Sarko D, Rice FL, Mann DA, Bauer GB (2011): Manatee vibrissae: evidence for a "lateral line" function. Ann NY Acad Sci 1225:101-109.

Renouf D (1979): Preliminary measurements of the sensitivity of the vibrissae of harbour seals (*Phoca vitulina*) to low frequency vibrations. J Zool 4:443-450.

Rice FL, Mance A, Munger B (1986): A comparative light microscopic analysis of the sensory innervation of the mystacial pad. I. Innervation of vibrissal follicle-sinus complexes. J Comp Neurol 252:154-174.

Rice FL (1993): Structure, vascularization, and innervation of the mystacial pad of the rat as revealed by the Lectin *Griffonia simplicifolia*. J Comp Neurol 337:386-399.

Ridgway S, Harrison R (1981): Handbook of Marine Mammals Volume 2: Seals. London, Academic Press.

Riedman M (1990): The Pinnipeds: Seals, Sea Lions, and Walruses. Berkeley, University of California Press.

Rybczynski N, Dawson MR, Tedford RH (2009): A semi-aquatic Arctic mammalian carnivore from the Miocene epoch and origin of Pinnipedia. Nature 458:1021-1024.

Sarko DK, Reep RL, Mazurkiewicz JE, Rice FL (2007): Adaptations in the structure and innervation of follicle-sinus complexes to an aquatic environment as seen in the Florida manatee (*Trichechus manatus latirostris*). J Comp Neurol 504:217-237.

Sarko DK, Leitch DB, Girard I, Sikes RS, Catania KC (2011): Organization of somatosensory cortex in the northern grasshopper mouse (*Onychomys leucogaster*), a predatory rodent. J Comp Neurol 519:64-74.

Sarko DK, Rice FL, Reep RL (2015): Elaboration and innervation of the vibrissal system in the rock hyrax (*Procavia capensis*). Brain Behav Evol doi:10.1159/000381415.

Savage RJG (1957): The anatomy of *Potamotherium* an Oligocene lutrine. J Zool 129:151-244.

Scheffer VB (1964): Hair patterns in seals (Pinnipedia). J Morphol 115:291–304.

Schwerdtfeger WK, Oelschläger HA, Stephan H (1984): Quantitative neuroanatomy of the brain of the La Plata dolphin, *Pontoporia blainvillei*. Anat Embryol 170:11-19.

Setzu A, Ffrench-Constant C, Franklin RJM (2004): CNS axons retain their competence for myelination throughout life. Glia 45:307-311.

Stenn KS, Zheng Y, Parimoo S (2008): Phylogeny of the hair follicle: the sebogenic hypothesis. J Invest Dermatol 128:1576-1578.

Stephens RJ, Beebe IJ, Poulter TC (1973): Innervation of the vibrissae of the California sea lion, *Zalophus californianus*. Anat Rec 176:421-441.

Stephens DW, Krebs JR (1986): Foraging Theory. Princeton, Princeton University Press.

Stephens PA, Carbone C, Boyd IL, McNamara JM, Harding KC, Houston AI (2008): The scaling of diving time budgets: insights from an optimality approach. Am Nat 171:305-314.

Szabo G (1958): The regional frequency and distribution of hair follicles in human skin; in Montagna W, Ellis RA (eds): The Biology of Hair Growth. New York, Academic Press, pp. 33–38.

Thewissen JGM, George J, Rosa C, Kishida T (2011): Olfaction and brain size in the bowhead whale (*Balaena mysticetus*). Mar Mamm Sci 27:282-294.

Uhen MD (2007): Evolution of marine mammals: back to the sea after 300 million years. Anat Rec 290:514-522.

Vincent SB (1913): The tactile hair of the white rat. J Comp Neurol 23:1-36.

Wathne J, Haug T, Lydersen C (2000): Prey preference and niche overlap of ringed seals *Phoca hispida* and harp seals *P. groenlandica* in the Barents Sea. Mar Ecol Prog Ser 194:233-239.

Welker WI, Johnson Jr. JI, Pubols Jr. BH (1964): Some morphological and physiological characteristics of the somatic sensory system in raccoons. Am Zool 4:75-94.

Wieskotten S, Dehnhardt G, Mauck B, Miersch L, Hanke W (2010): Hydrodynamic determination of the moving direction of an artificial fin by a harbor seal (*Phoca vitulina*). J Exp Biol 213:2194-2200.

Winkelmann RK (1959): The innervation of a hair follicle. Ann NY Acad Sci 83:400-407.

Woolsey TA, Van der Loos H (1970): The structural organization of layer IV in the somatosensory region (SI) of mouse cerebral cortex: The description of a cortical field composed of discrete cytoarchitectonic units. Brain Res 17:205-242.

Yablokov AV, Klevezal GA (1962): Whiskers of whales and seals and their distribution, structure, and significance; in Kleinebergh SE (ed): Morphological Characteristics of Aquatic Mammals.Translation Number 1335, Fisheries Research Board of Canada. Ste Anna de Bellevue, pp 48-81.